MODELLING AND SIMULATION OF STANDALONE PV SYSTEM WITH BATTERY STORAGE

A DISSERTATION

SUBMITTED IN PARTIAL FULFILLMENT OF THE REQUIREMENTS

FOR THE AWARD OF THE DEGREE

OF

MASTER OF TECHNOLOGY

IN

POWER SYSTEM

Submitted by:

SAURABH THAKRAN

Roll No. 2K16/PSY/15

Under the supervision of

Prof. Rachana Garg

DEPARTMENT OF ELECTRICAL ENGINEERING

DELHI TECHNOLOGICAL UNIVERSITY

(Formerly Delhi College of Engineering)

Bawana Road, Delhi-110042

2018

DEPARTMENT OF ELECTRICAL ENGINEERING

DELHI TECHNOLOGICAL UNIVERSITY

(Formerly Delhi College of Engineering)

Bawana Road, Delhi-110042

CERTIFICATE

I, Saurabh thakran, Roll No. 2K16/PSY/15 student of M.Tech. Power System (PSY), hereby declare that the dissertation/project titled **"Modelling and simulation of standalone PV system with battery storage"** is a bonafide record of work carried out by me under the supervision of Prof. Rachana Garg of Electrical Engineering Department, Delhi Technological University, Delhi in partial fulfillment of the requirement for the award of the degree of Master of Technology has not been submitted elsewhere for the award of any Degree.

Place: Delhi

Date:

Saurabh Thakran

Prof. Rachana Garg

(Supervisor)

Professor

Department of Electrical Engineering

Delhi Technological University

ACKNOWLEDGEMENT

I am highly grateful to the Department of Electrical Engineering, Delhi Technological University (DTU) for providing this opportunity to carry out the project work.

I would like to thank my supervisor Prof. Rachana Garg, Department of Electrical Engineering for her support, motivation and encouragement throughout the period this work was carried out. Her readiness for consultation at all times, her educative comments, her concern and assistance even with practical things have been invaluable.

I would like to express a deep sense of gratitude and thanks to Prof. Madhushudan Singh for providing the laboratory and other facilities to carry out the project work.

I would also like to thank to Ms Nikita Gupta and Ms Pallavi Verma (research scholars of electrical engineering department DTU), my batchmates and friends who encouraged and helped me in completing the dissertation.

Finally, I would like to expresses gratitude to all faculty members of Electrical Engineering Department, DTU for their intellectual support throughout the course of this work.

SAURABH THAKRAN

2K16/PSY/15

M. Tech. (POWER SYSTEM)

Delhi Technological University

ABSTRACT

As the population is increasing and quality of life is becoming better, demand for energy is also increasing and fossil fuel resources are depleting. Moreover, the use of fossil fuel causes pollution and global warming. These concerns leads to the worldwide adoption of renewable sources of energy viz. solar energy, wind energy, geothermal energy etc. Renewable energy sources do not cause harm to the environment and can be used repeatedly. Solar energy is the most widely used renewable energy source. Solar PV array is the most critical part of a standalone PV system. In this work modelling and design of standalone PV system is studied.

Solar energy produced by the photovoltaic array varies, as atmospheric conditions changes. MPPT controllers are used to obtain the maximum power from the PV array under various atmospheric conditions. These controllers work on Maximum power point tracking algorithms (MPPT). There are many MPPT algorithms described in literature. In this work five such algorithms viz. Fractional open circuit voltage, Perturbation and Observe, Incremental conductance, Fuzzy logic and Adaptive neuro-fuzzy Inference system(ANFIS) MPPT algorithms has been studied and a comparative analysis is presented.

PV array works only when there is sunlight. So during night or cloudy or rainy conditions PV array does not provide required power. For providing the power under these conditions energy storage systems viz. ultra-capacitors, batteries etc. are used. In this work batteries as energy storage element is studied. The batteries in standalone PV system are charged during the day and provide power to the load at night. In this work battery charging scheme for PV system is designed and analysed. To further get an insight about battery charging, a battery charging scheme using AC supply is designed. AC battery chargers find applications in Electric vehicles, households etc.

TABLE OF CONTENTS

LIST OF FIGURES

LIST OF TABLES

ABBREVIATIONS

AC	Alternating current
ANFIS	Artificial neural network-fuzzy
CAGR	Compound annual growth rate
CC	Constant current
CC-CV	Constant current-constant voltage
CV	Constant voltage
EV	Electric vehicle
FF	Fill factor
FLC	Fuzzy logic
FOCV	Fractional open circuit voltage
INC	Incremental conductance
ISA	International solar alliance
LED	Light emitting diode
MPPT	Maximum power tracking
P&O	Perturbation and observe
PV	Photovoltaic
SRISTI	Sustainable Rooftop Implementation for Solar Transfiguration of India

LIST OF SYMBOLS

C_1	Storage Capacitor
$C_{f,,max}$	Filter Capacitance
C_o	DC Link Capacitor
f_s	Switching Frequency
G_n	Nominal Irradiance
I_d	Diode Current
I_{pk}	Maximum Value of Peak Current
I_{PV}	Photovoltaic Current
I_{sc}	Short Circuit Current
L_o	Output Inductor
L_s	Source Inductance
R_p	Parallel Resistance
R_s	Series Resistance
V_{oc}	Open Circuit Voltage
ΔI_L	Inductor Ripple Current
ΔV_c	Capacitor Ripple Voltage
Θ	Fundamental Displacement Angle
ω	Operating Frequency

CHAPTER I
INTRODUCTION

INTRODUCTION

The increasing energy demand, decline in fossil fuel resources and concerns over climate change like global warming make the alternative and renewable source of energy fascinating worldwide. A renewable energy source is a resource which can be used repeatedly and replaced naturally. The renewable energy includes biomass, geothermal energy, wind energy, hydropower and solar energy.

Solar energy is one of the most widely used form of renewable energy. It is the energy provided by sun in the form of light and heat. The heat provided by the sun, as solar thermal energy, is used for solar heating. The sunlight is used in photovoltaics for generation of electrical energy.

Photovoltaic (PV) as a renewable energy source shows a significant growth in recent years. Over the period of 15 years, the production of solar PV has highly shoot-up with a compound annual growth rate (CAGR) of more than 40 % that makes this sector as one of the fastest growing ones in the world. Global PV installed capacity has reached 401.5 GW by 2018[1]. India too has shown tremendous growth in PV installations as shown in Fig 1.1.

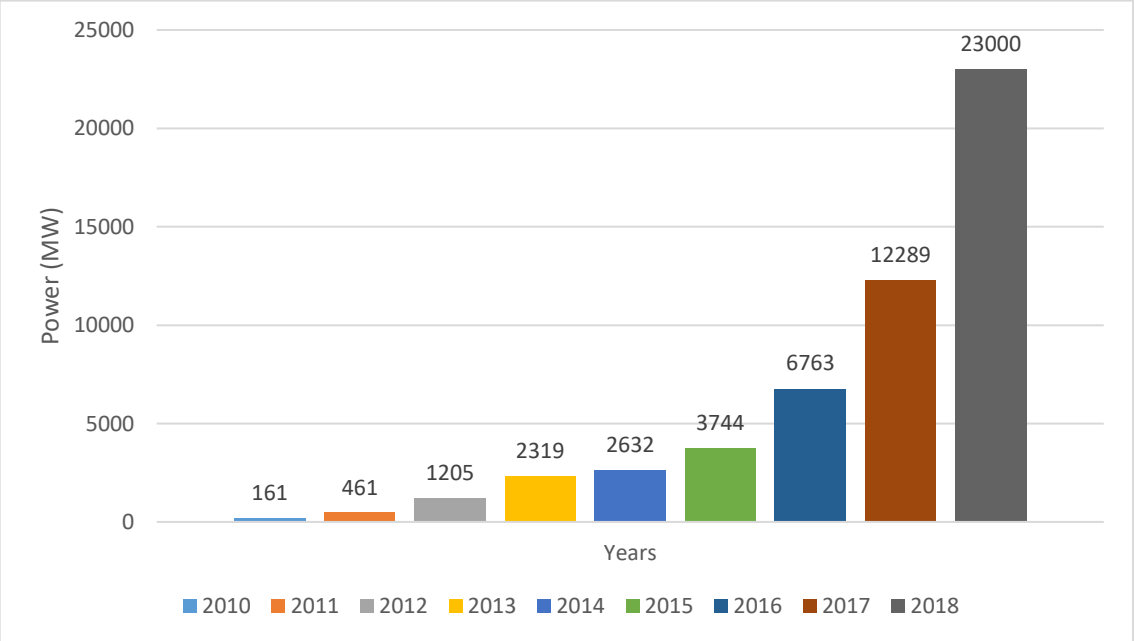

Fig 1.1 Photovoltaic installed capacity in India [2]

In 2010 India had an installed capacity of 161 MW and has reached 23GW in June 2018.This capacity was initially targeted to achieve by GOI till 2022 but it was achieved four years before the schedule period as 3GW was added in 2015-16, 5GW was added in 2016-17 and approx. 10GW was added in 2017-18 [3].

1.1 SOLAR ENERGY BASED INITIATIVES IN INDIA

The government of India started National Solar Mission in 2010 to encourage solar energy. In this initiative a target of 20 GW PV installations by 2022 was set which was later increased to 100 GW by 2022 in 2015. In this initiative the use of off grid solar PV installation is promoted for local energy needs, where there is no grid connectivity [3].

Sustainable Rooftop Implementation for Solar Transfiguration of India (SRISTI) scheme was proposed by government in 2017 for promoting rooftop power installations in India. Under this scheme, government will provide subsidy for rooftop solar installations. The generation target of 40 GW by 2022 from solar rooftop is set. The government proposed to spend Rs. 23,450 crores for this scheme [4].

The government of India, on 05-June-2017, has passed a proposal for retrofitting over 10 lakh traditional street light by solar-powered LED-based streetlight in Andhra Pradesh [3].

The government of India has also launched capital subsidiary scheme in 2014 for building up solar Photovoltaic water pumping system meant for irrigation purposes [3].

International Solar Alliance (ISA) was formed in 2015, for effective utilisation of solar energy. It consists of 121 countries having high solar potential. The objective of this alliance is to reduce dependence on non-renewable energy sources [4].

1.2 MOTIVATION

The use of solar energy is increasing day by day and government also have a keen focus on developing standalone PV systems for effective usage in various sectors like rural electrification, agriculture, solar rooftop for residential applications etc. Further, the use of dc based loads such as LED light, mobiles, computer, BLDC motor etc. is increasing. The biggest challenge in standalone PV system is the usage of solar panel up to its maximum efficiency at various conditions of solar irradiation and temperature, as the solar PV output is intermittent and inconsistent. This challenge can be overcome by designing a suitable power tracker, which can extract maximum power from standalone PV system under given conditions of irradiation and temperature. Battery is a crucial part

of standalone PV system. For appropriate and safe charging of battery, a battery charger is required. A battery charger helps to charge the battery quickly and safely by maintaining the current and voltage within limits.

1.3 OBJECTIVES

The primary objective of this thesis work is to model and design a standalone PV system for dc loads with battery storage. MPPT is used to extract the maximum power from the designed PV array. Also, an efficient and fast battery charging scheme has been designed. Photovoltaic power is produced by the photovoltaic array varies as the atmospheric conditions changes. There are two forms of photovoltaic systems, namely grid connected and standalone. In grid connected systems, the energy produced by the photovoltaic array feeded to the electricity grid. In this form the PV system does not require any energy storage. The standalone PV systems are autonomous systems and are not connected to grid, so standalone PV system requires energy storage to balance the PV generation and load demand.

Standalone PV systems produce power independent of the main grid and commonly used in areas that are outside the reach of the electricity grid. Applications of standalone PV systems in remote areas include lighthouse operation, remote communication stations and water pumps. PV array generates power only when sunlight is available. At night or during cloudy conditions standalone PV system failed to provide required power. So a battery storage system is a critical part of standalone PV system. PV array charge the battery during daytime, when sunlight is available and during night or cloudy conditions battery supply the load. In this work MATLAB/Simulink model of standalone PV system having maximum power point tracking capability is developed. The performance of standalone PV system using various maximum power tracking algorithms viz FOCV, P&O, INC, FLC, ANFIS are analysed. Also a battery charging scheme for standalone PV system is designed in MATLAB/Simulink and its performance is analysed. Further, battery charging system using AC supply is also designed and simulated using MATLAB/Simulink.

1.4 ORGANISATION OF THESIS

This dissertation has been arranged in six chapters. The first chapter introduces the significance of solar energy, motivation and objectives of this work.

Chapter 2 covers the literature review of the research work undertaken in the field of standalone PV system, battery charging system and associated areas.

Chapter 3 describes the components of standalone photovoltaic system. This chapter includes the basic description of DC-DC converters, MPPT systems and battery charging schemes.

Chapter 4 describes various maximum power point tracking algorithms. The simulation studies has been carried out and a comparative analysis of the MPPT techniques has been presented.

Chapter 5 describes battery charging systems. Battery chargers based on photovoltaic and AC supply are designed in MATLAB/Simulink and their performance are analysed.

Chapter 6 presents the summary of the dissertation and conclusion, as well as the future scope of this work.

1.5 CONCLUSION

This chapter describe briefly about solar energy scenario in India, standalone PV system and government initiatives for promoting solar energy. This chapter also provide a brief introduction of the topics discussed in the work. Also, the objective of this work and organisation of thesis is presented.

CHAPTER II

LITERATURE REVIEW

INTRODUCTION

This chapter aims to provide a concise literature review of standalone PV system, battery charging system and related areas. For the presented work, brief surveying of previous literature research work has been done in context with design of DC-DC converter, maximum power point tracking techniques (MPPT) and battery charging systems. The prime emphasis of this literature review is on the following topics:

i. Modelling of standalone PV system.
ii. Maximum power point tracking algorithms.
iii. Battery charging systems

2.2 MODELLING OF STANDALONE PV SYSTEM [5-15]

The major components of standalone PV system are PV array, DC-DC converter and batteries including its charging system.

M. G. Villalva et al.[5] presents a method of design and simulation of solar PV array to obtain the of the current voltage equation through regulation of the curve at three places i.e. open circuit, maximum power point, and short circuit.

Zadeh et al. [6] has validated that photovoltaic cell exhibits the non- linear characteristics which depend on the solar irradiation and some environmental factors. The author discussed the mathematical modelling of photovoltaic cells with respect to environmental conditions and analysed the performance for photovoltaic cell and conclude that a controller is needed to extract maximum power from photovoltaic cell.

Augustin McEvoy et al.[7] gives a complete overview of grid interfaced SPV systems, which includes characteristic curves, grid-interfaced configurations, various inverter topologies (both for single and three phase system), control techniques, maximum power point tracking (MPPT) algorithm, and ways to detect anti islanding.

Baharudin et al. [8] discussed the role of Solar PV as an excellent sustainable energy and it is in very much in demand nowadays. The authors presented the different topologies of different converter that can be integrated with PV panels. A comparative analysis of buck, boost, and buck-boost converters has been presented on the basis of cost, efficiency, limitations and no. of components used.

Putri et al. [9] discussed the advantages of Solar PV as it's an unlimited energy but have low efficiency. So to increase the efficiency of the photovoltaic array the authors operate PV on MPP using MPPT techniques. The authors discussed about different DC-DC converter that can be used with MPPT to control its switching and concluded that the buck converter has better efficiency and have fewer components than other. The authors also discussed the designing equation of inductance and capacitance of buck converter that has been feasible for battery charging.

2.3 MAXIMUM POWER POINT TRACKING ALGORITHMS [16-26]

Gosumbonggot [16] discussed about the variation in output power generated from solar panels with respect to the irradiation changes. So to minimize these variations in the system the author uses buck converter whose duty is controlled by perturb and observed algorithm. So using P&O algorithm the system can easily track under variable conditions. The result presented by author described that using MPPT method the accuracy of the system increases with respect to the load voltage.

Himanshu Sekhar Sahu et al. [17] explains the power generation by the PV modules at different levels of solar irradiation. The power generated varies with the variation in solar irradiation level.

Sera et al.[18] presented the two mainly used MPPT algorithms i.e. P&O and INC methods. The authors gave the literature for the both algorithm which clarify the misconceptions therefore useful in selecting the efficient algorithm for research purposes. The author analyzed the both algorithm under dynamic and static conditions.

Wibowo et al. [19] explained that efficiency of the PV system depends on temperature and irradiation. So to track the maximum power under the variable conditions the system require MPPT. Among various MPPT algorithms the author implemented Perturbation & observe and incremental conductance that are most widely used MPPT algorithms. The author uses buck-boost converter and its duty is controlled by two MPPT algorithms separately and the author also compare its results which proved that the INC method for power tacking is superior to P&O and has lower oscillations.

Tey & Mekhilef [20] has explained the modification that can be implemented incremental conductance algorithm under partial shading conditions. As in partial shading conditions the conventional MPPT algorithm fail to track MPP and the authors also discussed the SEPIC converter and its duty cycle is controlled by modified MPPT control. The author

analysed that modified INC for partial shading conditions able to track MPP rapidly and accurately.

Algazar et al. [21] has proposed a soft computing technique for tracking the maximum power point of solar PV system under the variable irradiation and temperature. The authors use a Cuk converter and its duty cycle has been controlled by fuzzy logic based MPPT controller. The results of fuzzy logic based MPPT is compared with the system which has been working without any MPP controller. From this comparison author analysed that fuzzy logic based MPPT work more efficiently and perform better under variable condition. The author uses Solar PV fed DC water pump to carry out this comparison.

Gupta et al. [22] described the fuzzy logic control and adaptive neural network MPPT algorithm and the authors compared these algorithms on the basis of their efficiency and their response to varying conditions i.e. irradiation and temperature. The author uses standalone PV system with resistive load for comparing both intelligent techniques. The authors concluded that the ANN has high tracking efficiency than FLC algorithm.

2.4 BATTERY CHARGING SYSTEM

2.4.1 Battery charging for PV systems [27-32]

M.E. Glavin et al. [27] explain the working of hybrid energy storage system consisting of valve regulated lead acid batteries and supercapacitors. The authors propose the application of energy storage system in Standalone PV system. In the proposed system the battery and the supercapacitor supply the average and instantaneous power to the load. The authors provide algorithm for a proposed controller. The proposed controller improves the life of battery by protecting battery from overcharging and deep discharging.

Lopez et al. [28] presented a battery charger for photovoltaic system. The PV system uses MPPT technique between battery bank and PV system. The author design buck converter and performed modelling of buck converter using bode plot analysis, voltage control & current control loop analysis for different modes of battery charging. The result shows the bulk charge, overcharge and float charge graph of battery charging. The authors analysed battery charging using digital signal processor (DSP).

Ala A. Hussein et al. [29] explains the design considerations of outdoor PV based battery charger. The authors also assesses the performance of PV chargers using various battery

chemistries. The author analyse that during varying environment conditions traditional charging methods fail to terminate charging when the battery is charged

2.4.2 Battery charging for electric vehicle (EV) [33-38]

Radha Kushwaha et al. [33] proposed the design of a battery charger based on power factor correction converter. The designed charger works on constant-current constant-voltage charging algorithm. The author proposes that the designed charger operate at high power factor and have low total harmonic distortion (THD). The charger has low ripple at the output and no detuning problem. The proposed system achieves the performance specifications given by IEC 61000-2 power quality standards.

Murat Yilmaz et al.[34] reviews the various battery chargers and power levels used for battery chargers. The authors analyse that unidirectional chargers require less hardware and provide better battery performance. The on board charger have the disadvantage as it provides limited power due to its weight and space constraints. The authors propose a strategy to overcome the disadvantages by using integral electric drive.

Ivan Subotic et al. [35] proposed a three phase battery charger for electric vehicle, using power electronic component present in the vehicle. The proposed charger works without any reconfiguration of hardware parts on vehicle. The charger uses additional degree of freedom present in nine phase machine to avoid electromagnetic torque production during charging process. The charger operates at unity power factor and no torque is produce in the machine during charging process. The proposed charger found application in systems where there are no asymmetries within each individual three-phase winding.

Deepak Gautam et al. [36] proposed the design of a 3.3kV two stage battery charger for plugin hybrid electric vehicle. The proposed design provides high efficiency and less charging time. The charger meets performance specifications of IEEE 1000-3-2 standard. The designed charger works at almost unity power factor and can operate for a wide range of voltage.

H. Bai et al. [37] explains the working two different battery charging algorithms and propose the design of 11kV battery charger. The proposed charger is designed using the principle of symmetric space vector pulse width modulation. The proposed charger utilise the zero voltage switching technique of DC-DC converter to obtain high efficiency. The proposed charger operates at high efficiency for a wide voltage range.

2.5 CONCLUSION

Significant amount of work has been done in the field of standalone PV system. This chapter covers a brief literature review of the work done so far on the relevant topics i.e. PV system, MPPT algorithms, battery charging based on photovoltaic array and grid supply.

CHAPTER III

MODELLING OF STANDALONE PV SYSTEM

INTRODUCTION

Standalone PV systems produce power independent of electricity grid. These systems are most widely used in remote areas that are outside the reach of electricity grid and where cost of grid extension is high. This chapter describes the components of the standalone PV system for dc loads and their mathematical models. The effects of variation of atmospheric conditions such as irradiation and temperature on power output of PV array and its I-V characteristics are discussed. The design and modelling of power electronic DC-DC converters has been presented. Also types of batteries and battery charging systems has been discussed.

3.2 COMPONENTS OF STANDALONE PV SYSTEM

The various components of standalone photovoltaic systems are photovoltaic array, maximum power point tracker, DC-DC converters and energy storage elements viz batteries, ultra-capacitors etc. as shown in fig 3.1.

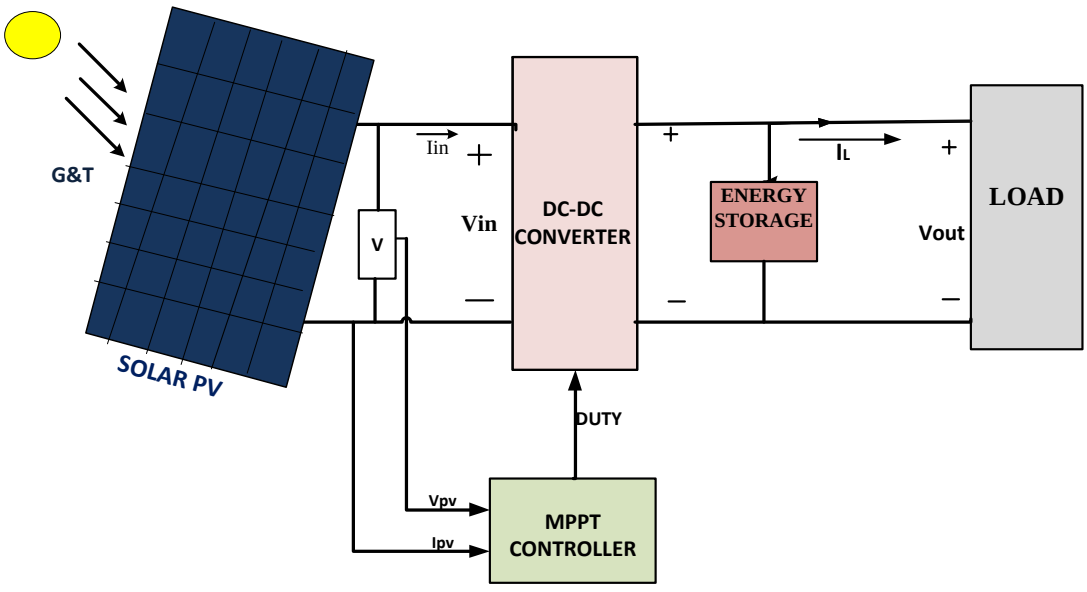

Fig 3.1 Block diagram of Standalone PV system

3.2.1. Photovoltaic Array

A photovoltaic array consists of solar modules connected in series and parallel. A solar module comprises of a number of photovoltaic cells. A photovoltaic cell is the basic unit

of a photovoltaic array. Photovoltaic cell converts solar radiation into dc electricity using the photovoltaic effect. The generation of voltage under the exposure of light in a material is called photovoltaic effect. It was first discovered by Edmond Becquerel in 1839[5].He illuminate the silver chloride connected to electrodes of platinum by placing it in acidic medium to obtain voltage and current. In the earlier days, photovoltaic cell was made up of Selenium bar. World's first photoelectric module made up of selenium was constructed by Charles fritts. But this module had an efficiency less the 1% [10]. In 1954 Calvin Fuller and Gerald Pearson of Bell Laboratories constructed the first practical photovoltaic cell made of Silicon. This cells had the efficiency of 2.3% [11]. Now the cell made of Gallium and Indium efficiency has reached to max level of 41.1% [12].

A PV cell is made up of P-N junction diode with P layer on the top, to facilitate the light photons to reach the P-N junction as shown in fig 3.2[13].The photons transfer energy to the valence electrons of P-N diode to make them eject from their atoms. Due to the vacancy created due to ejection of electrons holes are created. The electrons and holes comprise the current produced by PV cell. The current produced depends on PV cell surface area and insolation.

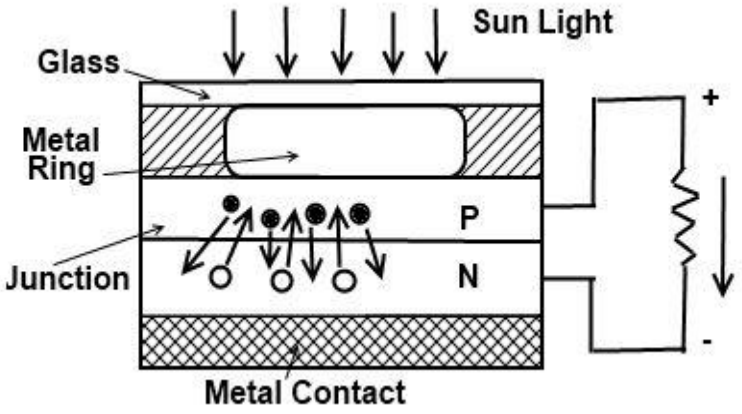

Fig 3.2 Construction of Photovoltaic cell[7]

To study the behaviour of photovoltaic cell, an electrical equivalent model using ideal electrical components is developed. An ideal PV cell is modelled as current source and a diode. However, in practice PV cells are not ideal, so to model them a shunt and a series resistance are added [5][7]. The single diode equivalent model of a single diode PV cell is shown in fig 3.3.

In the electrical equivalent a current source generates the photocurrent I_{PV}, which depends on the incident solar radiation and temperature. The diode represents the p-n

junction of the cell. The series resistor R_S and the parallel resistor R_P represent the losses in the PV cell. R_S denote the internal resistance of the cell. The parallel shunt resistor R_P characterises the leakage current of the p-n junction [7]. The net output current of the PV cell is the difference between the photocurrent I_{PV} and the diode current I_D.

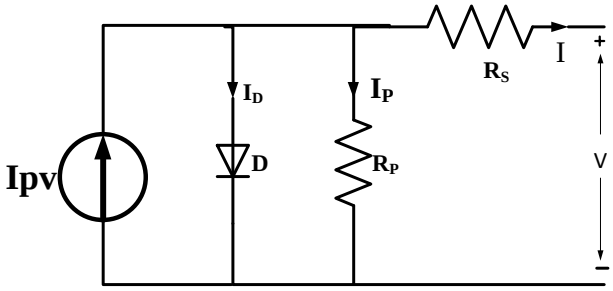

Fig 3.3 Single diode equivalent model of Photovoltaic cell [8]

Mathematically I–V characteristic of a PV cell is given by equation (3.1)

$$I = I_{pv,cell} - I_{o,cell}[e^{\left(\frac{qV}{\alpha kT}\right)} - 1] \tag{3.1}$$

The basic equation (3.1) of the photovoltaic cell does not provide the characteristics of a practical photovoltaic array. In practical photovoltaic array cells are connected in series and parallel. Series connected cell increase the output voltage and parallel connected cells increase the output current in photovoltaic array [12][13].For representing a practical array additional parameters to the basic equation are required. The net current produced by the photovoltaic cell is given by equation (3.2) and equation (3.3):

$$I = I_{pv} - I_D - I_P \tag{3.2}$$

$$I = I_{pv} - I_o\left[e^{\left(\frac{q(V+IRs)}{N_S KT}\right)} - 1\right] - [\frac{V+IRs}{Rp}] \tag{3.3}$$

Where I_O is the saturation current, N_s is the number of PV cells in series, K is boltzman constant, q is charge of an electron, I_{PV} is photovoltaic source current, , I_D is the diode current, Rs is the series resistance, Rp is the parallel resistance and I_P is the current through parallel resistance.The assumption $I_{sc} \approx I_{pv}$ is generally used in the modeling of practical photovoltaic arrays as practical PV arrays have low series resistance and high parallel resistance[12]. The saturation current in the diode is given by

$$I_o = \frac{I_{sc,n}+K_i\Delta T}{\exp\left(\frac{q(V_{oc,n}+K_v\Delta T)}{\alpha KT}\right)-1} \tag{3.4}$$

The saturation current I_o depends on temperature and its value increases with increase in temperature [5][13]. This equation (3.5) gives the current in PV array by taken into account the effect of temperature:

$$I_{pv} = (I_{pv,n} + K_i \Delta T) \frac{G}{Gn} \quad (3.5)$$

Where G is the irradiance at given time and G_n is the nominal irradiance at STC. Photovoltaic I-V and P-V characteristics shows the current vs voltage and PV output power vs voltage curves of a PV cell, module or array. These curves indicate the ability of PV cell, module or array to convert solar power to electrical power at various atmospheric conditions [15]. The knowledge of electrical characteristics of a photovoltaic cell or array is crucial for selection of PV array.

Fig 3.4 demonstrate the I-V characteristics and P-V characteristics of a PV array having Maximum power 680 W. These characteristics curves are obtained at standard test conditions (STC) (Irradiation of 1000W/m^2 and temperature of 25^{o}C). The characteristics obtained shows the maximum power point (MPP), Isc and Voc of PV array used.

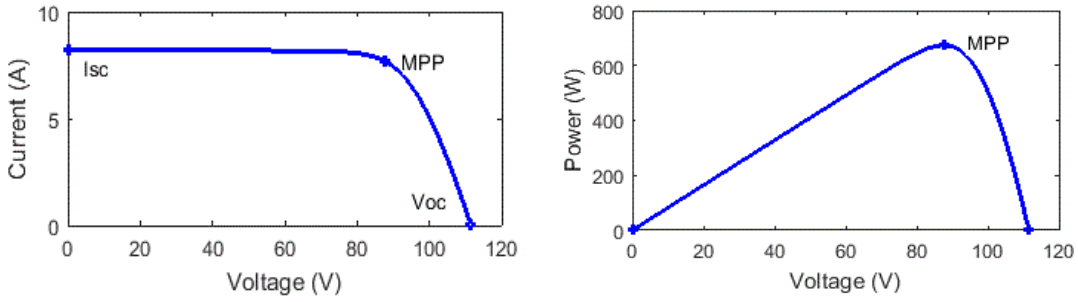

(a) (b)

Fig 3.4 (a) I-V characteristic (b) P-V characteristic of 680 W PV array at STC

Various parameters and terms necessary for analysing the characteristics of PV array are described below:

a) Solar Array Parameters

Open-circuit voltage (V_{oc}): It is the voltage produced at the terminals of PV array, when no load is connected across it [10].The value open circuit voltage is much higher than V_{mp} .

- **Short-circuit current (I_{sc}):** It is the current produced by PV array when its output are short circuited [10].The value of short circuit current is much higher than $I_{mp.}$

- **Maximum power point (MPP)**: It is the point where the power produced by the array is maximum when the array is connected with the load i.e. it can be batteries, DC load, Inverters. The MPP is the product of maximum voltage (V_{mp}) and maximum current (I_{mp}). It is measured in Watts (W) [7].
- **Fill factor (FF)**: The fill factor is the ratio of the maximum power that array can generate under operating conditions to the product Voc and $I_{sc.}$ The typical value of fill factor varies from 0.7-0.8 [7]. The fill factor gives an idea of the quality of the PV array, if the value of FF is unity the power provides by array will be more.
- **Efficiency**: The efficiency of a PV array is the ratio of the max. electrical power that the PV array can produced compare to the quantity of solar irradiance thrashing the array. The efficiency of a typical PV array is low i.e. around 10-12% and depends upon the type of cells being used in the array [7].

PV array datasheets provide information about the parameters of PV cell in nominal condition or standard test conditions (STC's) of temperature and solar irradiation. In this work a 680 W solar array with 5 series Kyocera KD135GX-LFBS module is used. The parameters of a module are shown in table 3.1.

Table 3.1 Parameters of Kyocera KD135GX-LFBS PV module

PV module parameter	**Value**
Open circuit voltage V_{oc}	22.3 V
Short circuit current I_{sc}	8.2 A
Cells per module N_s	36
Current at MPP I_{mp}	7.71 A
Voltage at MPP V_{mp}	17.5 V
Power at MPP P_{max}	134.925 W
R_p	254.76 Ω
R_s	0.2914 Ω
K_v	-0.1230 V/K
K_i	0.0032 A/K
I_0	$2.6417*10^{-8}$ A
Series connected modules per string	5
Number of parallel strings	1

The characteristic for a typical 680W array for varying level of solar radiations are given by fig 3.5(a) and fig 3.5(b). From the characteristics curves it can observed that I_{sc} and I_{max} decrease as the irradiation level reduces while V_{oc} remains nearly the same. Similarly, fig 3.6(a) and 3.6(b) shows the characteristic at varying temperature. It can be observed from the characteristic curves that as the temperature increases, V_{oc} and P_{max} decreases while temperature variation have little effect on I_{sc} of PV array[12][13].

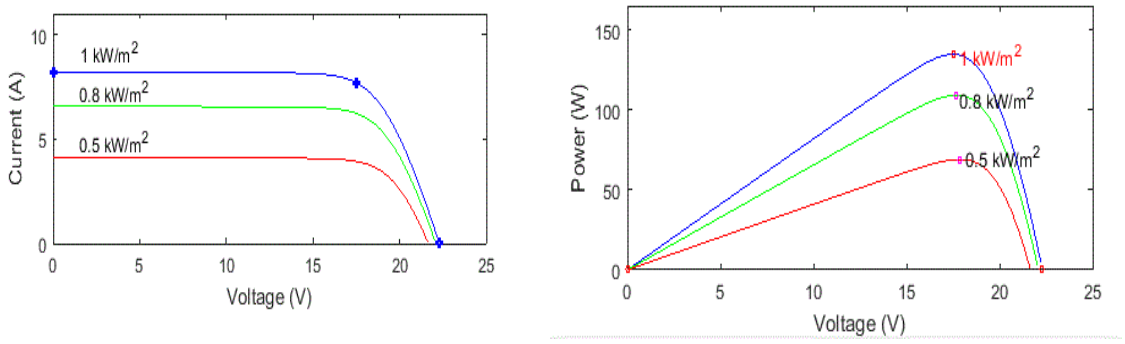

(a) (b)

Fig 3.5 (a)Voltage vs current characteristics (b) Power vs voltage characteristics for varying level of solar irradiations

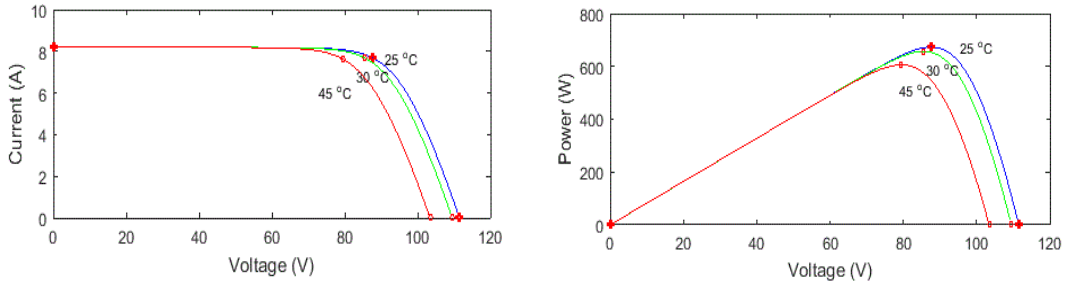

(a) (b)

Fig 3.6 (a)Voltage vs current characteristics (b) Power vs voltage characteristics at various temperature

3.2.2 DC-DC Converter

DC-DC converters are power electronic devices used to convert DC voltage at one level to required voltage level [8]. A DC-DC converter uses a semiconductor switches (MOSFET,IGBT etc.),The switch connect and disconnect the load from source giving a pulsating voltage output from a constant dc supply. For switching the MOSFET of DC converter a pulse of variable width is used [8][9]. In standalone PV system, MPPT

controller is used to change the pulse width of MOSFET switch to obtain maximum power. A DC-DC converter can be classified by ratio of output voltage to input voltage into following categories:

a) **Buck Converter**: It is a device used to reduce the input dc voltage to a lower output voltage. A buck converter can be shown by fig 3.7(a)It is mainly used in battery charging, brushed motor controller and power audio amplifiers etc.

b) **Boost converter**: It is a device used to increase the input dc voltage to a higher output voltage. A boost converter can be shown by fig 3.7(b).It is mainly used in regulated DC power supplies, regenerative braking of DC motor etc.

c) **Buck-Boost converter**: It can convert input dc voltage to higher or lower voltage than input depending on duty ratio. It can be shown by fig 3.7(c)It is mainly used in self-regulating power supplies, power amplifiers and adaptive control applications.

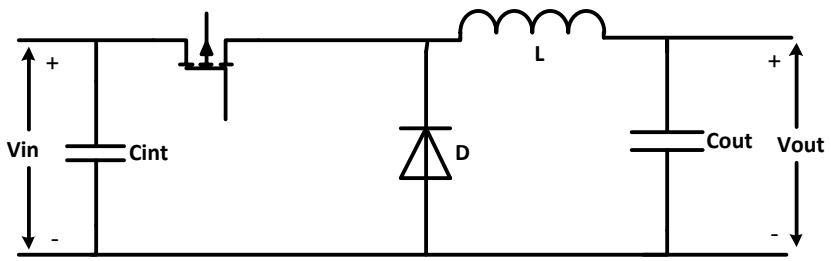

Fig 3.7(a) Circuit diagram of buck converter

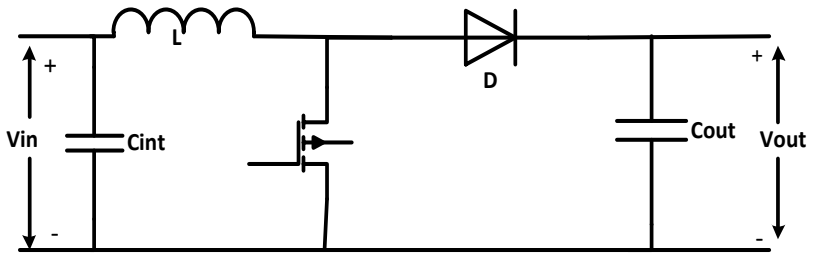

Fig 3.7(b) Circuit diagram of boost converter

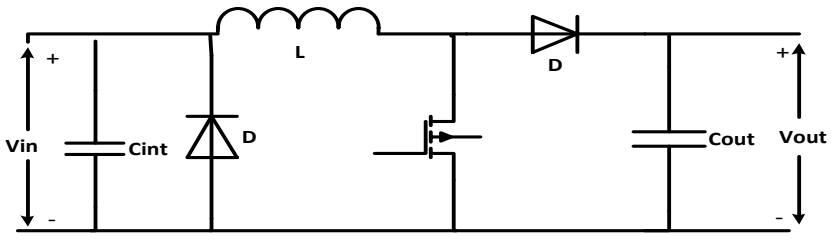

Fig 3.7(c) Circuit diagram of buck boost converter

3.2.2.1 Design of Buck converter [8][9]

In the present work, buck converter is used to stepdown the 87.5 V obtained from solar PV array to 48V at the output. A buck converter can be designed as:

a) MOSFET switch selection

MOSFET switch is selected based on load current, input and output voltage, switching frequency and the allowable power dissipation in switch [14]. In this work IRF 540 MOSFET is used which has a current rating of 30 A and the switch operate at a switching frequency of 25 kHz. The duty ratio required for the switch is given by equation (3.6)

$$\text{Duty (D)} = \frac{Vout}{Vin} = \frac{48}{87.5} = 0.55 \quad (3.6)$$

Where V_{in} is input voltage of the buck converter and V_{out} is voltage output at the battery

b) Inductor design

In a DC-DC converter, inductor is used to reduce the ripples in the output current waveform [14][15]. The inductor is designed based on equation (3.7)

$$\text{Inductance (L)} = \frac{D(1-D)Vin}{f_S.\Delta I_L} = \mathbf{1}.45\text{mH} \quad (3.7)$$

Where D is duty ratio of the converter, V_{in} is the voltage input, f_s is switching frequency and ΔI_L is inductor ripple current, 10% of converter output current.

c) Output Capacitor design

The output capacitors are used to minimize voltage variations [14] [15]. The value of output capacitor is given by equation (3.8)

$$\text{Capacitance (C)} = \frac{D(1-D).Vin}{8.f_s{}^2 L\Delta V_C} = 503.34\ \mu\text{F} \quad (3.8)$$

Where D is the Duty ratio of the converter ,V_{in} is input voltage, f_s is switching frequency, L is the inductance value, ΔV_c is capacitor ripple voltage is taken as 3% of $V_{in.}$ In this work output capacitor of 560 µF is used.

d) Input capacitor design

The input capacitance can be calculated by using equation (3.9) [15]

$$C_{in} \geq \frac{D(1-D)Io}{\Delta V_{in(p-p)} f_S} = 5.638\mu\text{F} \quad (3.9)$$

Where D is duty cycle of converter, $\Delta V_{in(p-p)}$ peak-to-peak value of input ripple voltage, f_s is switching frequency of the switch and I_o is maximum load current. In this work input capacitor of 6 µF is used.

3.2.3 Maximum power point tracking algorithm

The power supplied by the photovoltaic system to a load depends on the load connected to the photovoltaic module. The highest power can be transferred from solar PV array to load when the load line crosses the I-V characteristics at MPP as shown in fig 3.8.

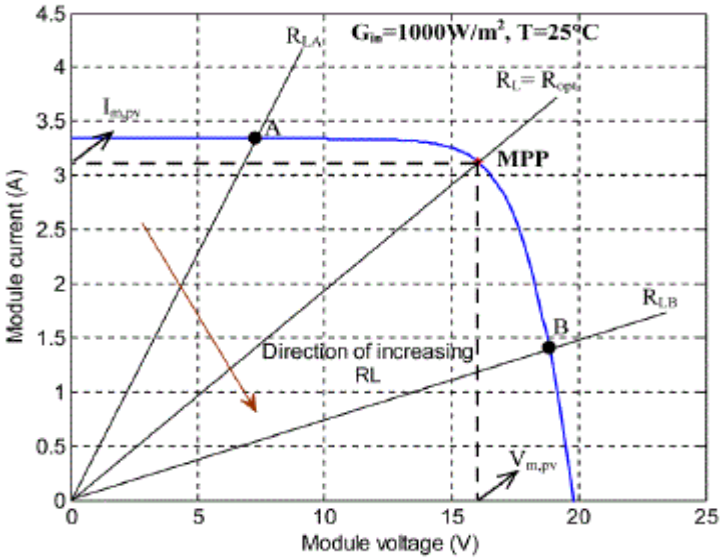

Fig 3.8 Operating point of PV module at resistive load [16]

MPPT controllers are used to obtain maximum power from solar photovoltaic modules. MPPT controllers vary the load impedance to match it with PV module impedance for given temperature and insolation conditions. The load impedance, as seen by PV array can be varied by varying the duty of MOSFET switch of DC-DC converter [16][23].

In buck converter the relation between output voltage and input voltage is given by equation (3.10) and the load impedance referred to input side of buck converter is given by equation (3.11)

$$Vo = D * V_{in} \tag{3.10}$$

$$R_i = \frac{R_L}{D^2} \tag{3.11}$$

Where D is the duty ratio, V_i is voltage at the input and V_o is voltage at the output and R_i is load impedance referred to input side of buck converter. The duty ratio of the buck

converter is varied to equate R_i with the internal impedance of PV module under given operating conditions to extract peak power.

Various MPPT algorithms have been developed so far. In the present work following MPPT algorithms are analyzed and compared.

a) Fractional over voltage algorithm
b) Perturb and observe algorithm
c) Incremental Conductance algorithm
d) Fuzzy logic algorithm
e) Adaptive neuro-fuzzy(ANFIS) algorithm

A detailed analysis of these MPPT algorithms is given in chapter 4.

3.2.4 Energy storage system

Energy storage devices store the energy produced to use at a later time. There are various energy storage devices used in standalone PV system, such as ultra-capacitor, battery and flywheel etc. Battery is the most widely used energy storage device in standalone PV system. Battery storage system consists of battery banks connected for storage of and plays important role in leveling the load and providing backup electricity in PV system. It improves the reliability of the overall system.

3.2.4.1 Battery technologies

There are various types of battery storage technologies available. Some of the most common battery technologies are Lead acid battery, NiMH battery, NaS battery and Li-ion battery [30]. A brief discussion of various battery technologies is given as follows:

a) Lead acid batteries

These batteries consist of positive and negative electrode of lead oxide and metallic lead, with sulphuric acid as electrolyte. These batteries can be classified into two types- Flooded lead acid batteries and sealed valve regulated lead acid (VRLA) batteries. Flooded leaded batteries are less expensive but they produce flammable gases [30]. The problem of flammable gases production is solved in VRLA batteries by using a valve, which facilitates recombination of hydrogen and oxygen. These batteries have the advantage of lower up front cost and higher efficiency.

b) NiMH batteries

These batteries have better energy densities than lead acid batteries. But it suffers from various disadvantages such as high self-discharge rate, limited service life and low columbic efficiency. These batteries are not ideal for fast charging; as large amount of heat is produced during fast charging along with hydrogen build up which may cause cell rupture leading to reduction in the capacity [31].

c) Li-ion batteries

In these batteries Li-ions are inserted into negative electrode and disinserted from positive electrode. During charging Li^+ is removed from cathode oxide and inserted into lattice of anode. These batteries have high energy density, high efficiency and long cycle life. Li-ion battery technology has made rapid development in the past decade leading to increasing cycle life and substantial price reduction.

d) NaS batteries

The NaS batteries are developed by ford motors for powering the early electric car models in 1960.The use of these batteries increases from 2002 for large scale energy storage. These batteries have energy density of 150-240Wh/kg, long lifetime (4000 cycles) and deep and fast discharge. These batteries have the ability to work at high temperature and harsh environment. Over the past decade these batteries played important role in supporting the renewable energy generation and power system. Comparison of various battery technologies are shown in table 3.2.

Table 3.2 Comparison of battery technologies [30]

Type of battery	Lead-Acid	NiMH	Li-ion	NaS	VRB
Energy density(Wh/kg)	25-50	60-120	75-200	150-240	10-30
Power density(W/kg)	75-300	250-1000	500-2000	150-230	80-150
Cycle life	200-1000	180-2000	1000-10000	2500-4000	>12000
Capital cost($/kwh)	100-300	900-3500	300-2500	300-500	150-1000

In this project Lead acid battery is used for energy storage application due to its cost effectiveness and reliability. The capacity of battery used in this project is 100Ah and the nominal voltage of the battery is 48V. Various parameters of the battery used are given as:

Table 3.3 Parameters of 100Ah Lead acid battery

Parameter	**Value**
Maximum Capacity(Ah)	104.1667 Ah
Nominal Voltage(V)	48 V
Cutoff voltage	36 V
Fully charged voltage	52.2632 V
Internal resistance	0.0048 Ω
Nominal Discharge current	20 A

The discharge characteristics of a 100Ah, 48V lead acid battery used in this work is shown in fig 3.8

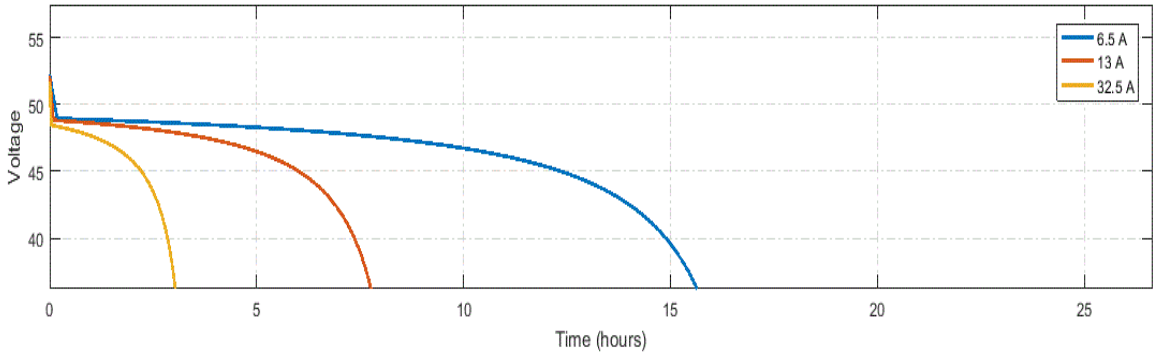

Fig 3.9 Discharge characteristics of 100 Ah battery at 6.5A,13A and 32.5 A

3.2.4.2 Battery Charge controller

A charge controller restricts the rate of current which is flowing through the electric batteries. It is used to protect the battery against overvoltage and may prevent against overcharging which can lessen the battery lifespan, and may create a safety risk. The charge controller also protect battery from excessive discharging, the current supplied by the battery and also protect its life [30][32]. The electronics circuit used for charge controller gives reliability and highest efficiency.

While the essential function of a battery charge controller is to avoid battery overcharging, numerous different functions may likewise be utilized, including low voltage load disconnect, control of backup power sources, load control. The charge controller must deal with the surge conditions required by the load or from the PV array that is connected to the controller. The sizing of the charge controller can be determined by multiplying the safety factor and the short-circuit current of the PV module.

3.3 CONCLUSION

This chapter discuss the various components of standalone PV system such as PV array, DC-DC converter, MPPT controller and battery storage system. The design of DC-DC converter and various topologies of battery charging controller is described.

CHAPTER IV

MAXIMUM POWER POINT TRACKING ALGORITHMS

INTRODUCTION

The output of solar PV array is intermittent in nature and depends heavily on atmospheric conditions like temperature and irradiation. The maximum power point trackers are controllers used to track the maximum power from a photovoltaic array under all the atmospheric conditions. These controllers vary the load impedance as seen by the PV array to match it with PV array impedance for given temperature and insolation conditions, so that the power transferred to the load is maximum [23]. These controllers vary the impedance by changing the duty ratio of gate signal of power MOSFET switch of the DC-DC converters.

4.2 MPPT ALGORITHMS

The MPPT controllers are one of the most important components of standalone PV system. These controllers use various parameter such as voltage, current, change in voltage, change in power etc. as inputs and by using appropriate algorithm obtain a duty ratio, required for extracting maximum power from PV array. Over the past decades many methods to find the MPP have been developed. This chapter describes and analyses five such maximum power point tracking algorithms namely:

i) Fractional open circuit voltage algorithm
ii) Perturb and observe algorithm
iii) Incremental conductance algorithm
iv) Fuzzy logic control (FLC) based MPPT algorithm
v) Adaptive neuro-fuzzy inference system (ANFIS) based MPPT algorithm

In this chapter MPPT algorithms are developed and simulated using MATLAB/Simulink and a comparison of all the developed algorithms have been presented.

4.2.1 Fractional open circuit voltage algorithm and Numerical results

The fractional open circuit voltage algorithm works on the observation that the maximum power point voltage of a photovoltaic (PV) array lies between 0.6 to 0.8 times to its open circuit voltage [23]. So in this algorithm the photovoltaic (PV) output voltage is

maintained at 0.6-0.8 times the open circuit voltage. This is implemented by proper switching of DC-DC converter connected at the output of PV array. However open circuit voltage of PV array varies as the temperature and insolation changes. Hence the fractional open circuit voltage (FOCV) MPPT algorithm does not work efficiently during varying atmospheric conditions.

The system consists of PV array, DC-DC buck converter as described in chapter 3.

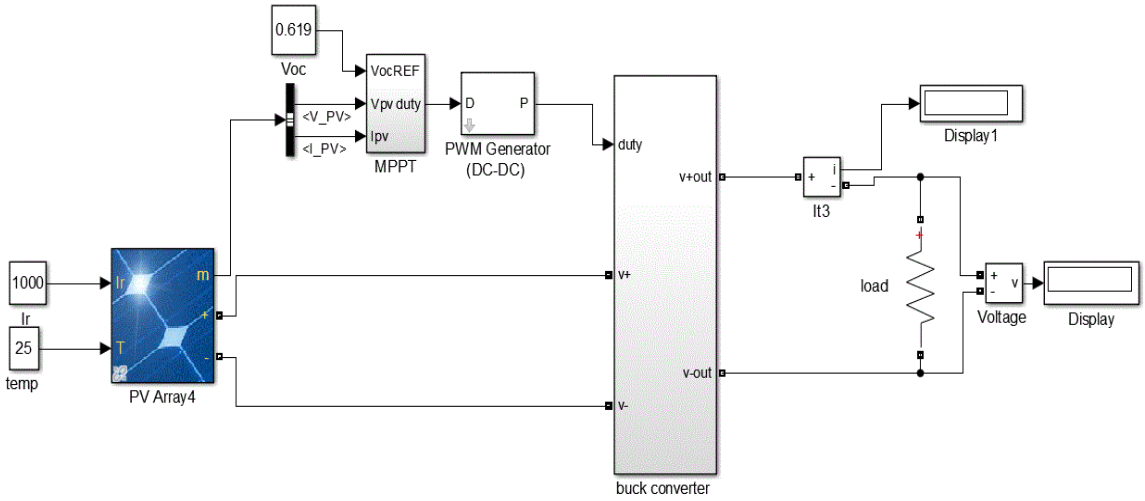

Fig 4.1 Simulink model of standalone PV system with fractional open circuit voltage MPPT algorithm

A MPPT control based on Fractional open circuit voltage algorithm is designed using Simulink/MATLAB. The performance of the algorithm is analysed for a 680W standalone PV system. Output power at the load under STC is 652.5 W as shown in fig 4.2. Voltage tracked by FOCV MPPT algorithm at STC is 47.25 V as shown in fig 4.3. Fig 4.4 gives the duty ratio.

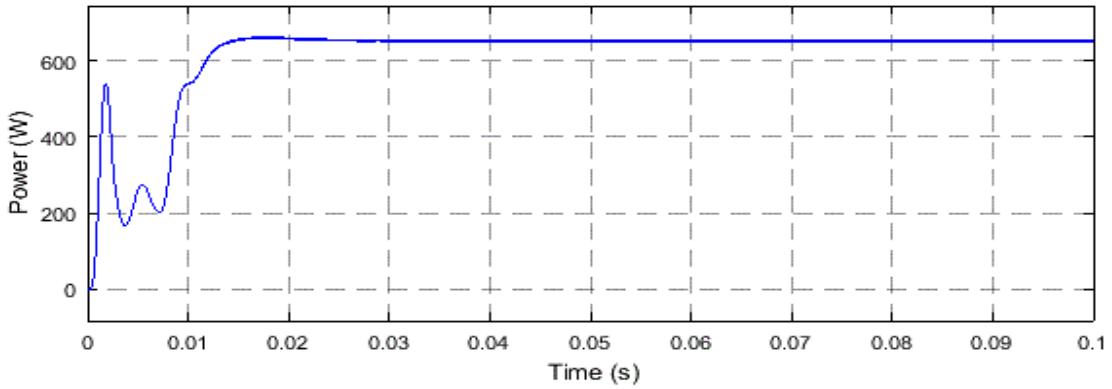

Fig 4.2 Power extracted using FOCV algorithm at STC

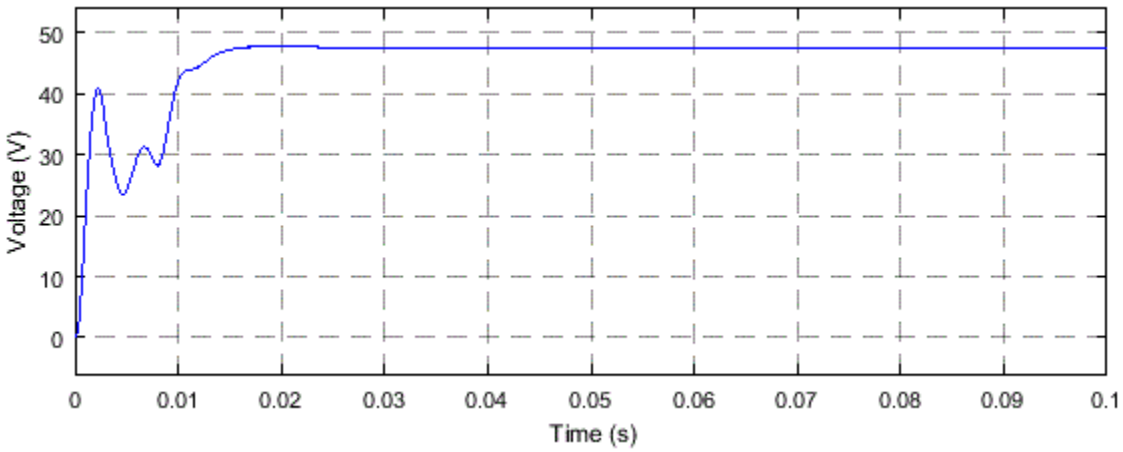

Fig 4.3 Voltage obtained using FOCV algorithm at STC

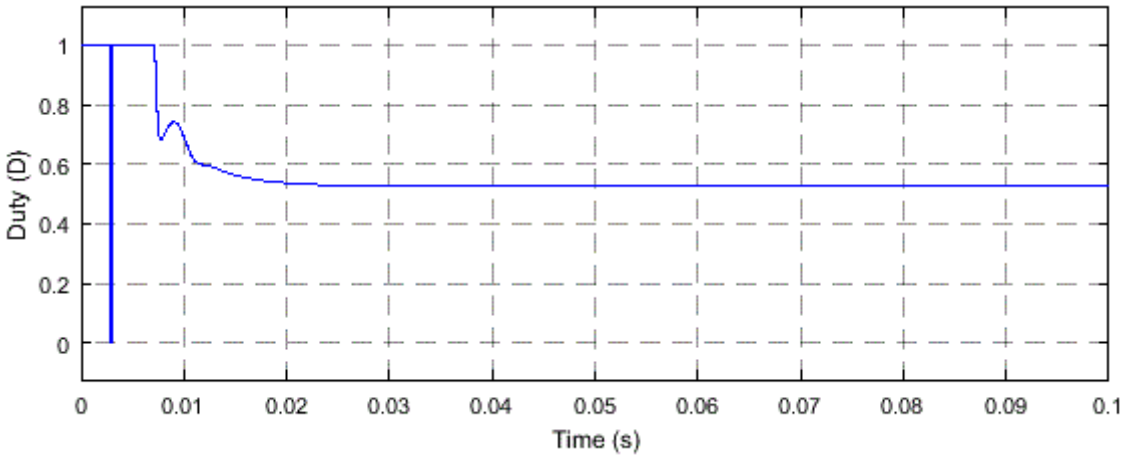

Fig 4.4 Duty ratio obtained at MPP using FOCV algorithm at STC

To analyze the effect of irradiation on the power output, the system is operated at varying irradiation and constant temperature of 25^0C. The irradiance is 1000W/m^2 up to 0.1 sec/800W/m^2 from 0.1 to 0.2 sec and 500W from 0.2 to 0.3 sec as shown in fig 4.5. The power extracted by FOCV MPPT algorithm is 652.5W, 532W and 335W respectively.

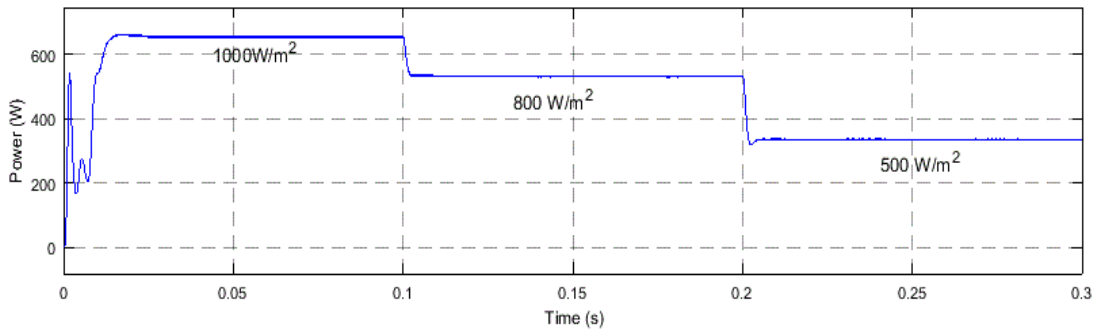

Fig 4.5 Power extracted using FOCV algorithm under varying irradiation condition

When the system is tested at the constant irradiance of 1000W/m^2 and at 25^0C for 0.1 sec, at 30^0C for 0.1 sec to 0.2 sec at 45^0C for 0.2 to 0.3 sec as shown in fig 4.6 then the

power extracted by FOCV MPPT controller are given by 652.5W,619W and 468W respectively.

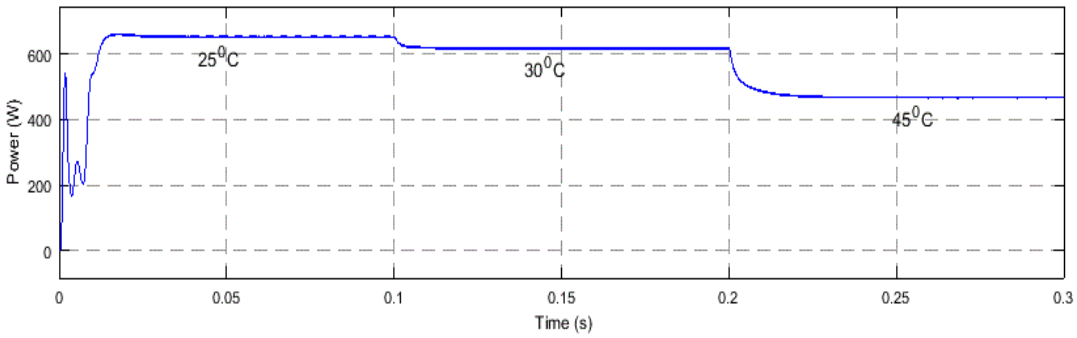

Fig 4.6 Power extracted using FOCV algorithm under varying temperature condition

4.2.2 Perturb and Observe Algorithm and Numerical results

In this method duty (D) is perturbed and resulting array current and voltage values are sensed, and accordingly power is calculated. Once the power is known, the slope of the P-V curve or the operating region is checked and duty ratio is perturbed. If power increases by increasing duty, then duty is increased further and if power decreases by increasing duty, then duty ratio is decreased. Similarly, if power increases by decreasing duty, then duty is decreased further and if power decreases by decreasing duty, then duty ratio is increased [16]. At MPP maximum power is obtained and if duty is perturbed further, power obtained reduces so direction of perturbation also reverses as shown in fig4.6. The algorithm oscillates around peak power point when stable condition is arrived [17][18]. The size of perturbation is kept small to keep the oscillation and the power variation small.

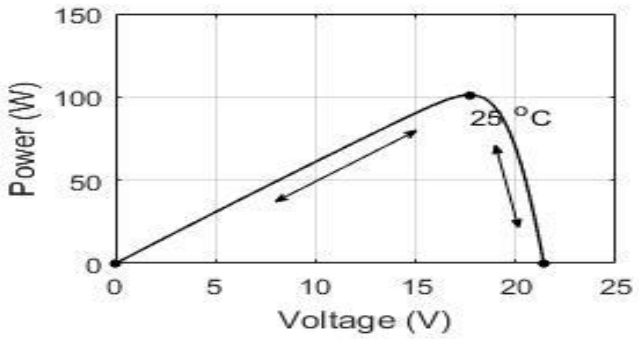

Fig 4.7 Variation of slope in power vs voltage characteristics

The flowchart of Perturbation and Observe algorithm is shown in fig 4.8

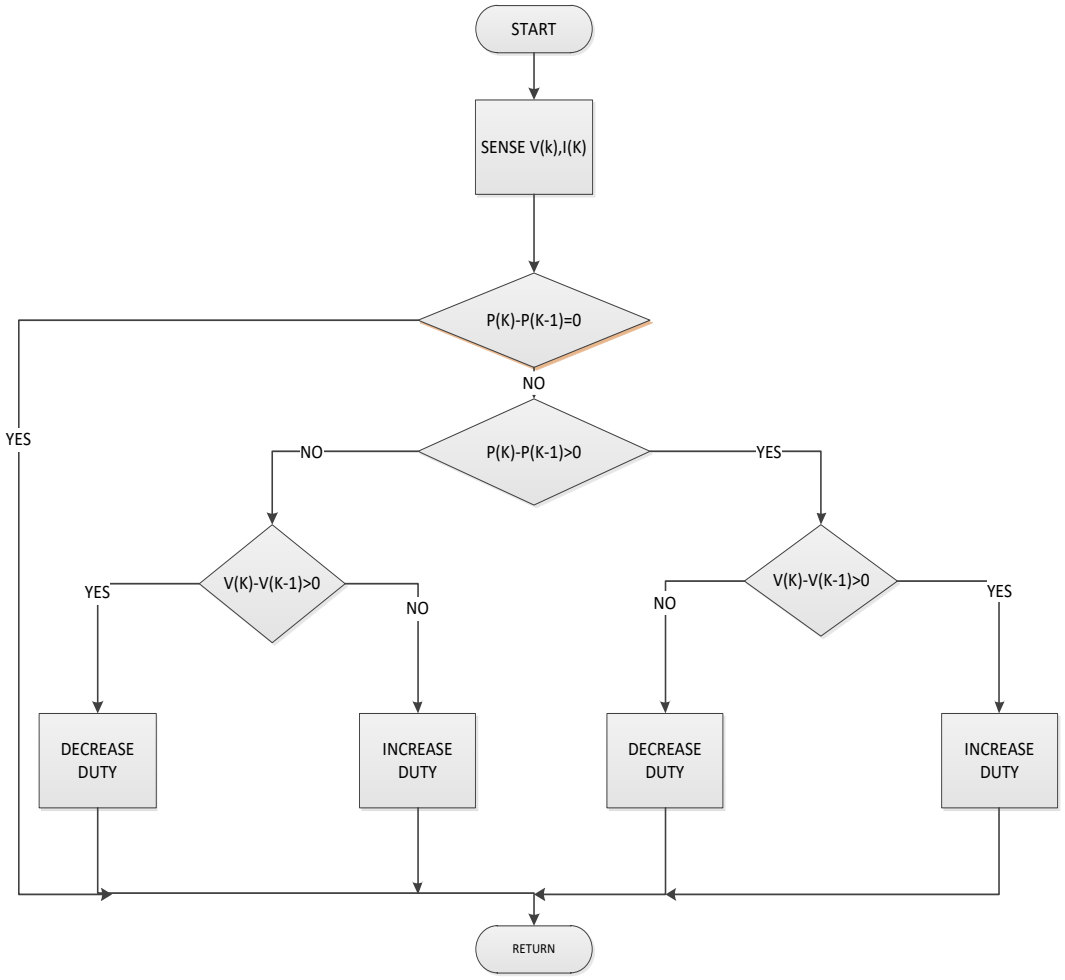

Fig 4.8 Flowchart of P&O Algorithm [19][20]

A MPPT controller based on Perturbation and Observe algorithm is designed using Simulink/MATLAB. The performance of the algorithm is analysed for a 680W standalone PV system. Output power at the load under STC is 660 W as shown in fig 4.9. Voltage tracked by P&O algorithm at STC is 47.6 V as shown in fig 4.10. Fig 4.11 gives the duty ratio obtained for maximum power.

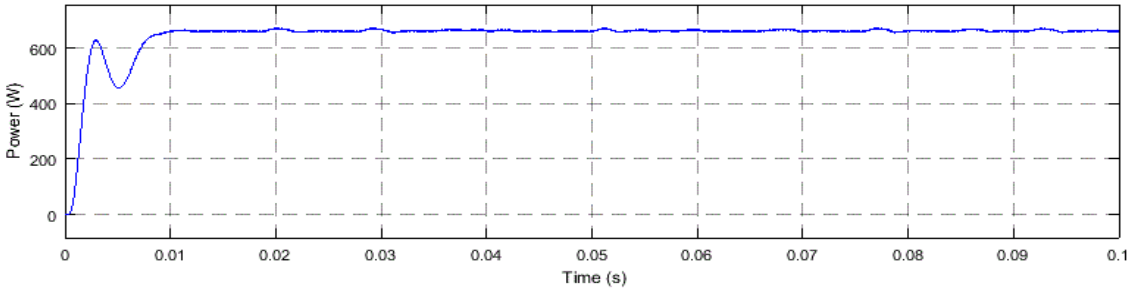

Fig 4.9 Power extracted using P&O algorithm at STC

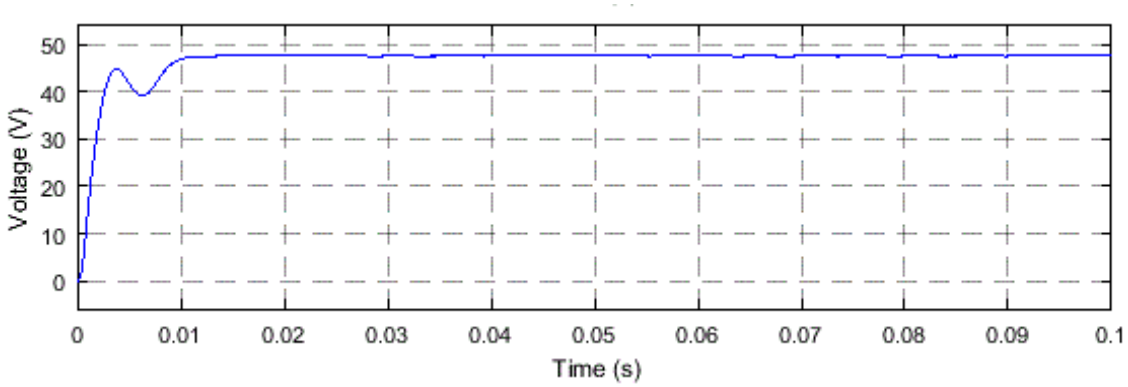

Fig 4.10Voltage obtained using P&O algorithm at STC

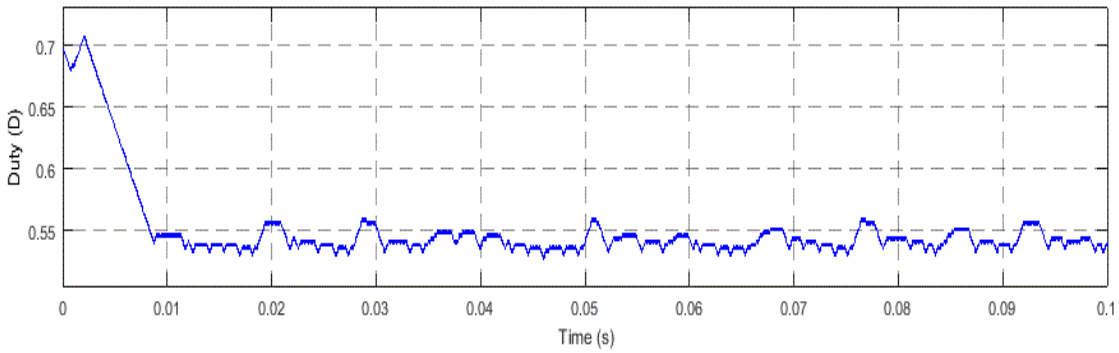

Fig 4.11Duty ratio obtained at MPP using P&O algorithm at STC

To analyze the effect of irradiation on the power output, the system is operated at varying irradiation and constant temperature of 25^0C. The irradiance is 1000W/m^2 up to 0.1 sec/800W/m^2 from 0.1 to 0.2 sec and 500W from 0.2 to 0.3 sec as shown in fig 4.12. The power extracted by P&O MPPT controller is 660W, 533W and 335W respectively.

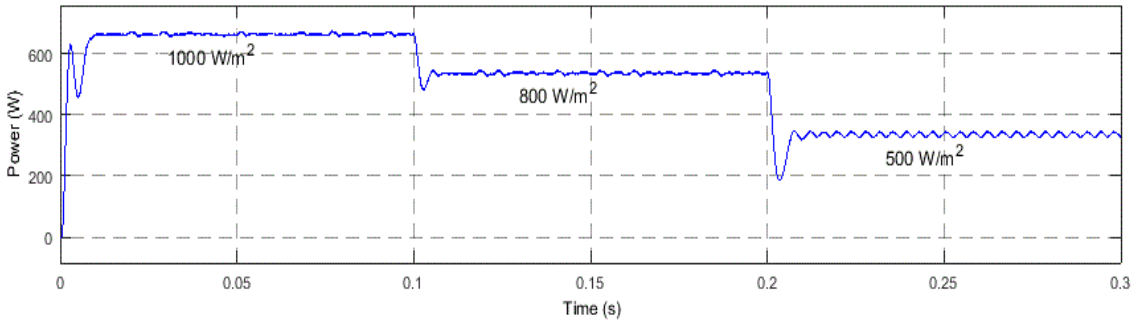

Fig 4.12 Power extracted using P&O algorithm under varying irradiation condition

To analyze the effect of temperature variation on the power output, the system is operated at varying temperature and constant irradiation of 1000W/m^2.The system is tested at the temperature of 25^0C up to 0.1 sec, at 30^0C from 0.1 sec to 0.2 sec and at 45^0C from 0.2

to 0.3 sec as shown in fig 4.13. The power extracted by P&O algorithm is 660W, 645W and 595W respectively.

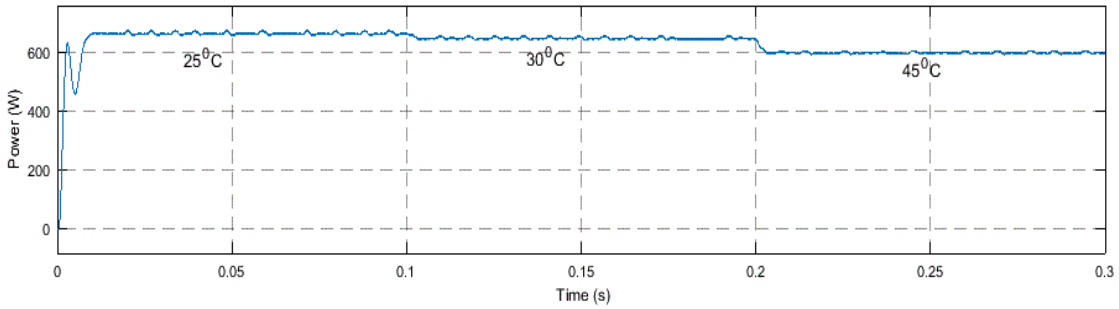

Fig 4.13 Power extracted using P&O algorithm under varying temperature condition

4.2.3 Incremental Conductance Algorithm and Numerical results:

This algorithm tracks the peak power point by measuring the incremental conductance of PV array. It works on the principle that the incremental conductance equals the instantaneous conductance at the point of maximum power [19]. At a point left to the maximum power on P-V curve, incremental conductance is more than instantaneous conductance and at a point right to the maximum power on P-V curve, incremental conductance becomes less than instantaneous conductance [20][23].

At MPP

$$\frac{dI}{dV} = \frac{-I}{V} \tag{4.1}$$

Left of MPP

$$\frac{dI}{dV} > \frac{-I}{V} \tag{4.2}$$

Right of MPP

$$\frac{dI}{dV} < \frac{-I}{V} \tag{4.3}$$

This MPPT controller measures the voltage and current of the PV array and calculate the conductance, then it changes the duty ratio of PWM pulse and calculate the rate of change of conductance or incremental conductance. Incremental conductance can be measured by measuring the slope of P-V characteristics of PV array. When the maximum power point is attained, then incremental conductance become same as instantaneous conductance [22][23]. The flow chart for this algorithm is shown in fig 4.14

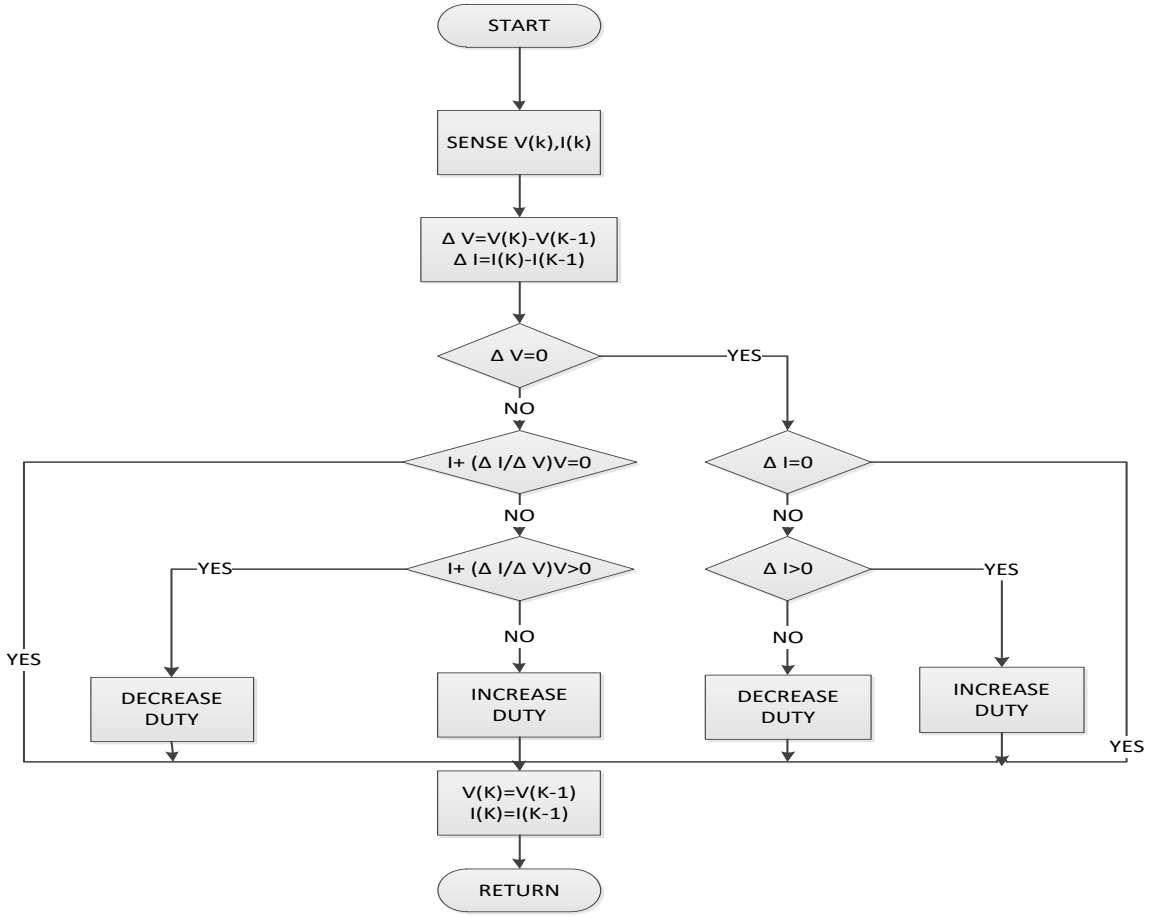

Fig 4.14 Flowchart of Incremental Conductance Algorithm

A MPPT controller based on Incremental conductance algorithm is designed using Simulink/MATLAB. The performance of the controller is analysed for a 680W standalone PV system. Output power at the load under STC is 659 W as shown in fig 4.15. Voltage tracked by INC MPPT controller at STC is 47.58 V as shown in fig 4.16. Fig 4.17 gives the duty ratio obtained for maximum power.

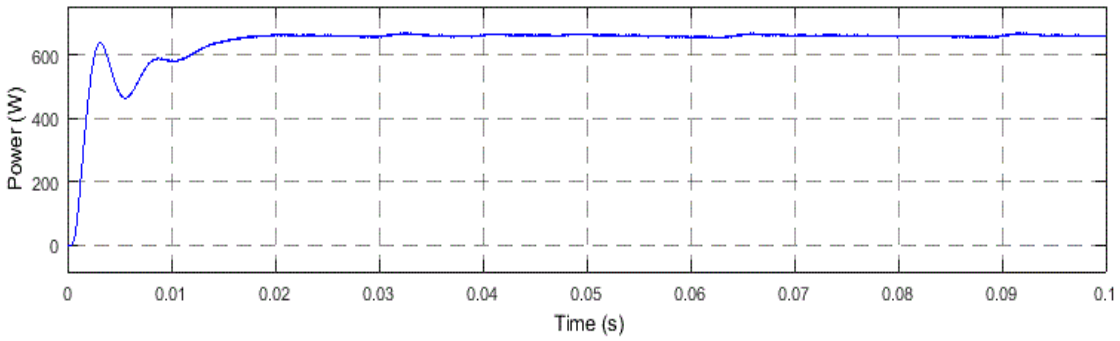

Fig 4.15 Power extracted using Incremental conductance algorithm at STC

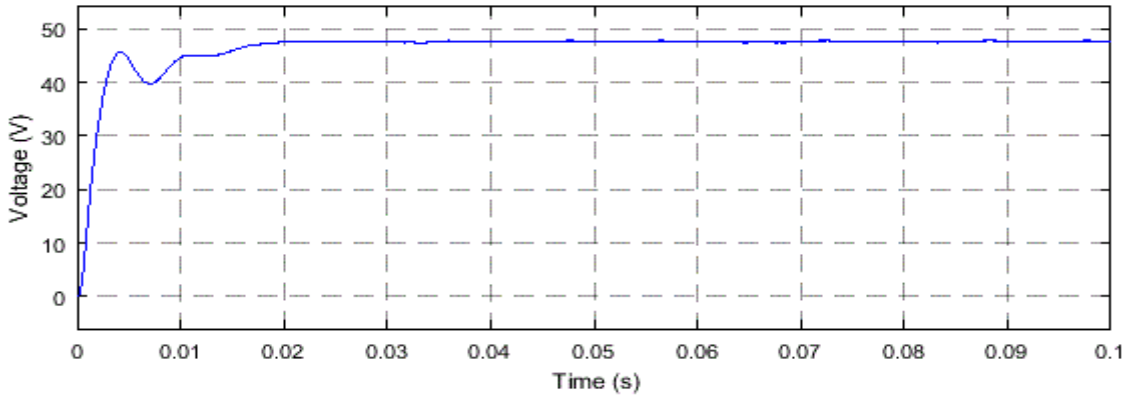

Fig 4.16 Voltage obtained using Incremental conductance algorithm at STC

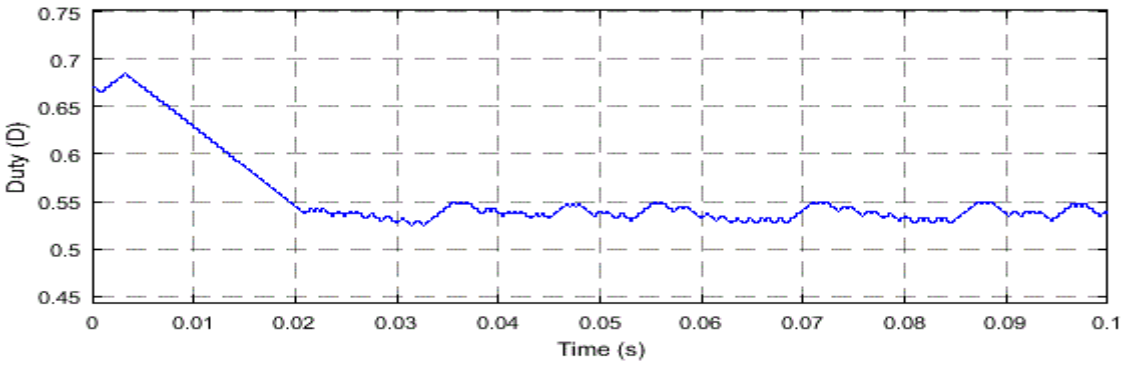

Fig 4.17 Duty ratio obtained at MPP using Incremental conductance algorithm at STC

To analyze the effect of irradiation on the power output, the system is operated at varying irradiation and constant temperature of 25^0C. The irradiance is 1000W/m^2 up to 0.1 sec/800W/m^2 from 0.1 to 0.2 sec and 500W from 0.2 to 0.3 sec as shown in fig 4.18. The power extracted by INC MPPT controller is 659W, 533W and 334W respectively.

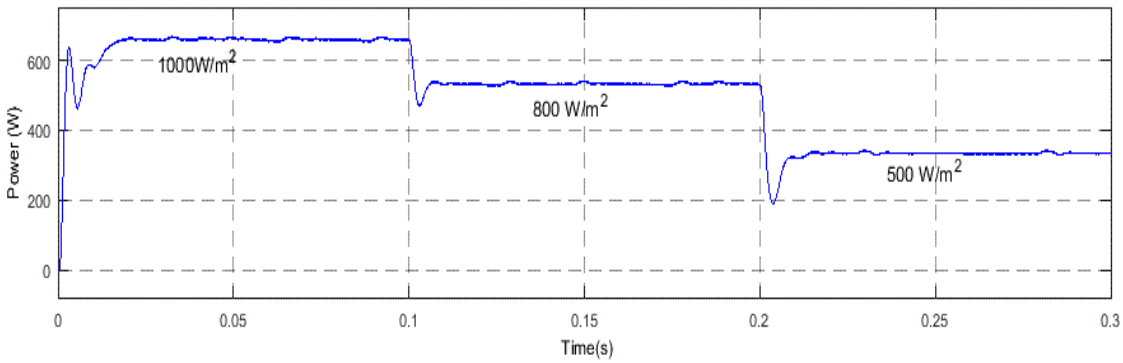

Fig 4.18 Power extracted using incremental conductance algorithm under varying irradiation conditions

To analyze the effect of temperature variation on the power output, the system is operated at varying temperature and constant irradiation of 1000W/m^2. The system is tested at the temperature of 25^0C up to 0.1 sec, at 30^0C from 0.1 sec to 0.2 sec and at 45^0C from 0.2

to 0.3 sec as shown in fig 4.19. The power extracted by INC MPPT controller is 659W, 644W and 594W respectively.

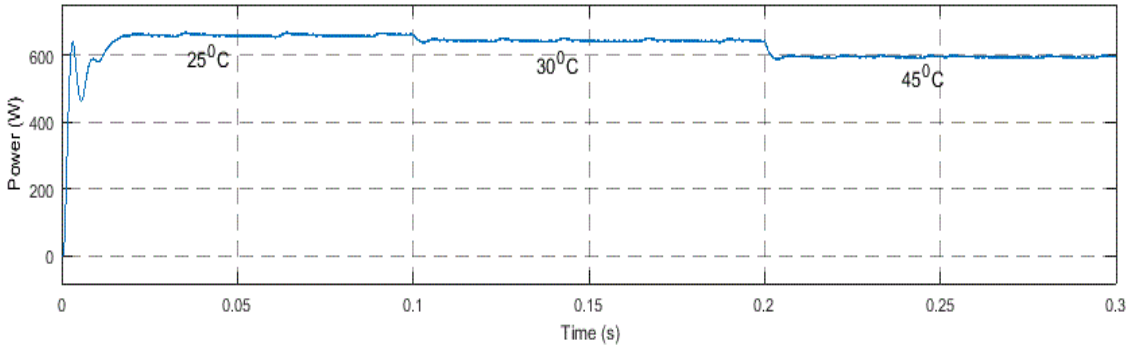

Fig 4.19 Power extracted using incremental conductance algorithm under varying temperature conditions

4.2.4 Fuzzy Logic Control based MPPT Algorithm and Numerical results:

This algorithm has the advantage of operating with general inputs, without any requirement of correct mathematical model of the system. Fuzzy logic based MPPT algorithm have three stages namely fuzzification, inferencing and defuzzification [21][22].

a) Fuzzification

In this stage, data input is converted into fuzzy sets using fuzzy variables and membership function. In the present work five different fuzzy levels viz. NB (negative big), NS(negative small), ZO(zero), PS(positive small), PB(positive big) are used for designing the fuzzy based MPPT controller. These levels are chosen, based on the range of input variables. The input variable to the fuzzy MPPT controller are generally taken as error (E) and variation of error (CE).The parameters used as E and CE are chosen based on convenience [22]. In this work the variable E and CE are expressed as follows:

$$E(k) = \frac{P(k)-P(k-1)}{I(k)-I(k-1)} \tag{4.4}$$

$$CE(k) = E(k) - E(k-1) \tag{4.5}$$

Where P(k) and I(k) are the power and current of the PV array, respectively. Therefore, E(k) shows rate of change of power with current, it also determine the location of operating point with reference to the maximum power point on P-I characteristics and CE(k) expresses the direction of movement of operating point. The output of the fuzzy MPP controller is generally given by duty ratio (D). The membership function of Fuzzy

MPPT algorithm are shown in fig 4.20. The change in duty ratio is obtained by applying fuzzy rule base based on the input to the fuzzy controller.

b) Inference Engine

The inference engine deduce the output of the fuzzy controller by applying fuzzy rules to the fuzzified input. Fuzzy rules are defined by user based on analysis of input variables. The fuzzy rules are shown in table 4.1, giving duty ratio for a given value of E and CE. The rule table consists of 25 fuzzy rules. There is a large variation in duty ratio, when the operating point is far away from the MPP and the variation is small, if the operating point is close to the MPP [22]. In the present work mamdani method is used for inferencing.

c) Defuzzification

The fuzzified duty ratio obtained from above have to be converted into crisp output. The duty ratio (D) thus obtained is used to control PWM of DC-DC buck converter for obtaining point of maximum power. There are two methods for defuzzification of fuzzy output namely Center of Area Method (COA) and the Max Criterion Method (MCM)[25][24]. The centre of gravity is used in this thesis for obtaining the centre of gravity (COA) of final combined fuzzy set. For a sample data representation, centre of gravity D is defined as

$$\Delta D = \frac{\sum_{j=1}^{n} \mu(\Delta D_j).\Delta D_j}{\sum_{j=1}^{n} \mu(\Delta D_j)} \tag{4.6}$$

The fuzzified output ΔD (k),is defuzzified and scaled by gain to give duty ratio *D* (*k*) as given by equation (4.7) :

$$D(k) = D(k-1) + S.\Delta D(k) \tag{4.7}$$

Where S is the gain.

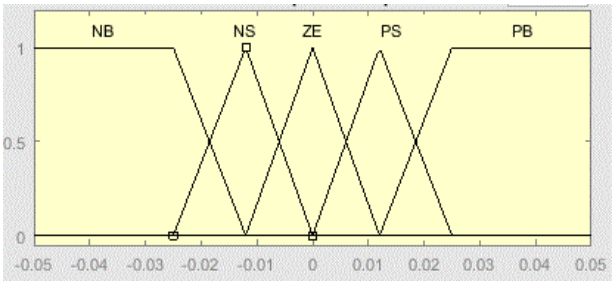

(a)

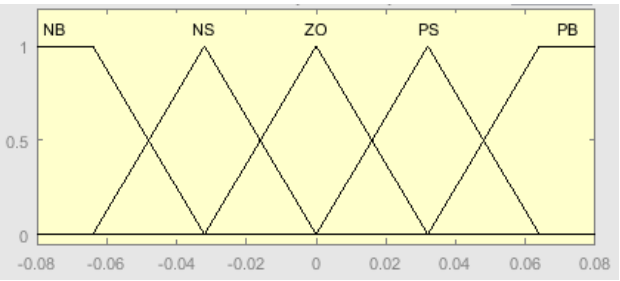

(b)

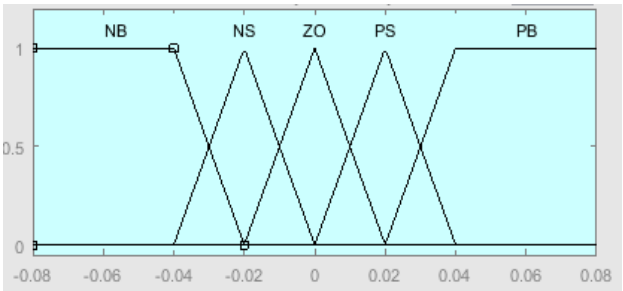

(c)

Fig 4.20 Membership functions of FLC a) Membership function for error b) Membership function for change in error c) Membership function for duty ratio

TABLE 4.1 FUZZY LOGIC RULE BASE

E / CE	NB	NS	ZE	PS	PB
NB	**PB**	**PB**	**ZO**	**NS**	**NB**
NS	**PB**	**PS**	**ZO**	**NS**	**NB**
ZO	**PS**	**PS**	**ZO**	**NS**	**NS**
PS	**PB**	**PS**	**ZO**	**NS**	**NB**
PB	**PB**	**PS**	**ZO**	**NB**	**NB**

A MPPT controller based on Fuzzy logic control based algorithm is designed using Simulink/MATLAB. The performance of the controller is analysed for a 680W standalone PV system. Output power at the load under STC is 663 W as shown in fig 4.21. Voltage tracked by based algorithm controller at STC is 47.65 V as shown in fig 4.22. Fig 4.23 gives the duty ratio obtained for maximum power.

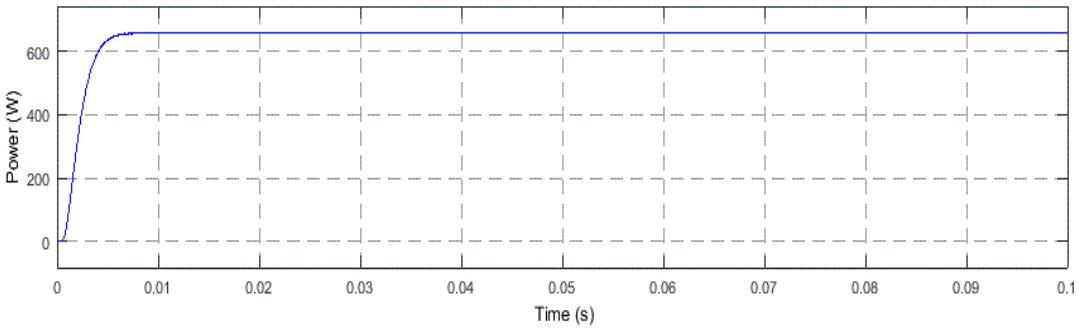

Fig 4.21 Power extracted using FLC based algorithm at STC

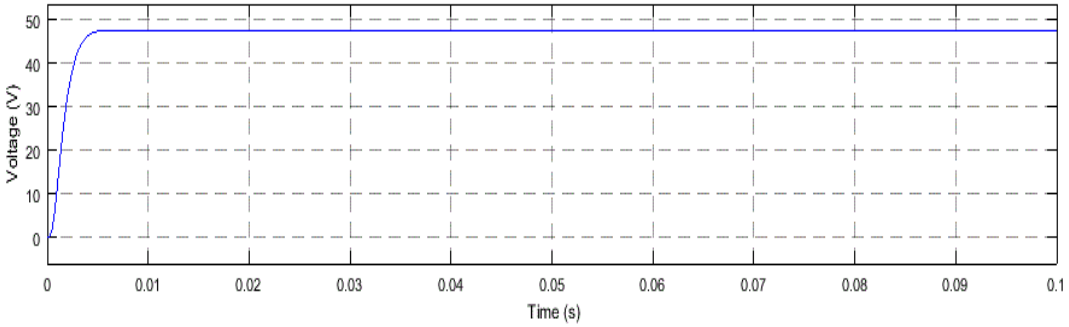

Fig 4.22 Voltage obtained using FLC based algorithm at STC

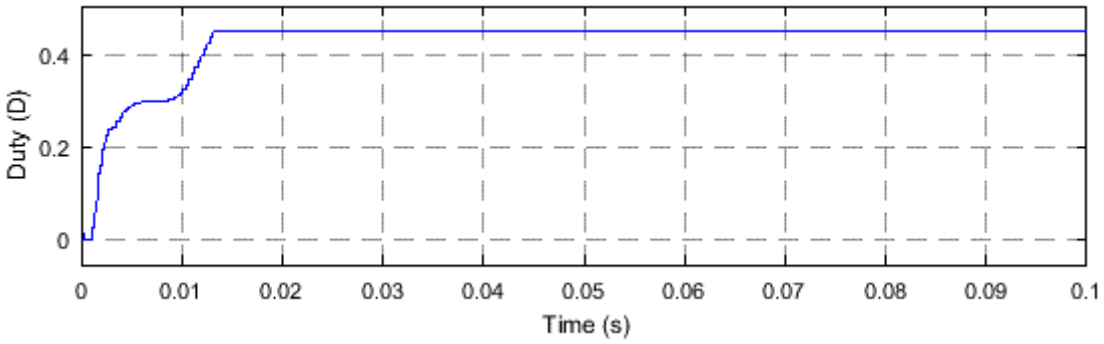

Fig 4.23 Duty ratio obtained at MPP using FLC based algorithm at STC

To analyze the effect of irradiation on the power output, the system is operated at varying irradiation and constant temperature of 25^0C. The irradiance is 1000W/m^2 up to 0.1 sec/800W/m^2 from 0.1 to 0.2 sec and 500W from 0.2 to 0.3 sec as shown in fig 4.24. The power extracted by FLC MPPT controller is 663W, 542W and 342W respectively.

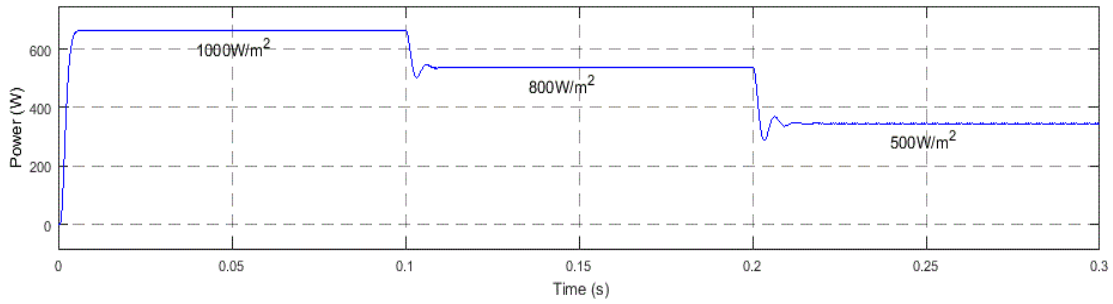

Fig 4.24 Power extracted using FLC based algorithm under varying irradiation conditions

To analyze the effect of temperature variation on the power output, the system is operated at varying temperature and constant irradiation of 1000W/m^2.The system is tested at the temperature of 25^0C up to 0.1 sec, at 30^0C from 0.1 sec to 0.2 sec and at 45^0C from 0.2 to 0.3 sec as shown in fig 4.25. The power extracted by FLC based algorithm is 663W, 648W and 597W respectively.

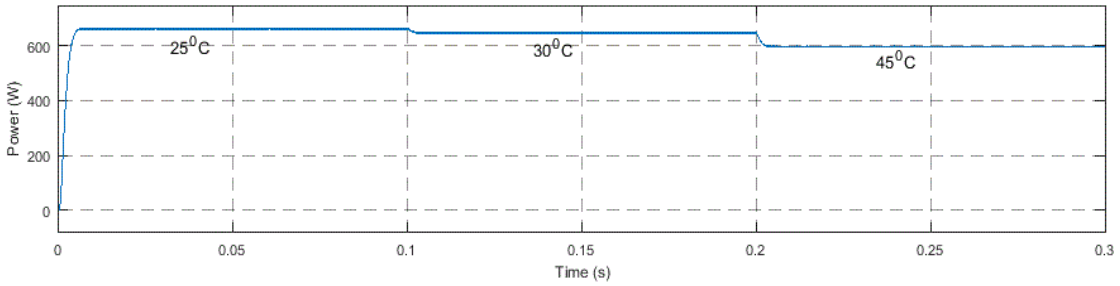

Fig 4.25 Power extracted using FLC based algorithm under varying temperature conditions

4.2.5 ANFIS based MPPT algorithm and Numerical results:

It is an AI based algorithm for MPP tracking. It uses both neural network and fuzzy logic to obtain maximum power point. A neural network consists of three layers given as input layer, hidden layer and output layers [23].Each layer of neural network has a number of data points known as nodes. The numbers of node vary from system to system and are defined by user. This helps the neural network to map the input output nonlinear function. However, neural network has a shortcoming that it cannot map heuristic terms. This shortcoming is not present in fuzzy logic which can map heuristic by using fuzzy rules and membership function but it requires prior knowledge of system for defining fuzzy rules and membership function [26]. The ANFIS integrate both these algorithms to obtain a hybrid and more accurate algorithm of maximum power tracking.

This algorithm uses voltage and current or irradiance and temperature as an input to the

ANFIS controller and the duty ratio is given as output. The accuracy of this algorithm depends on how well the algorithm is trained [27].

In the present work ANFIS MATLAB toolbox is used for designing and testing the algorithm. The voltage and current of photovoltaic array is used as input. A set of 180 values is used to train the algorithm in MATLAB toolbox. Based on the knowledge obtained from training data, membership function is selected.

During training phase of the algorithm the shape of membership function varies and a final shape is obtained at the end of training. The final algorithm obtained after training is used for tracking the maximum power.

Fig 4.26 (a) shows the structure of proposed ANFIS model and Fig 4.26(b) shows the training error of model.

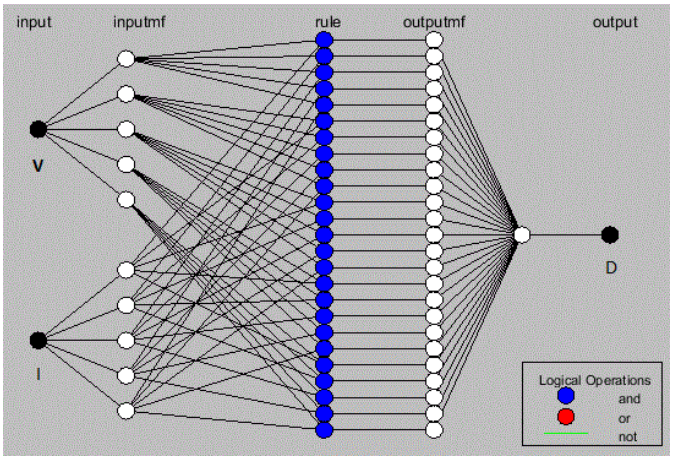

(a)

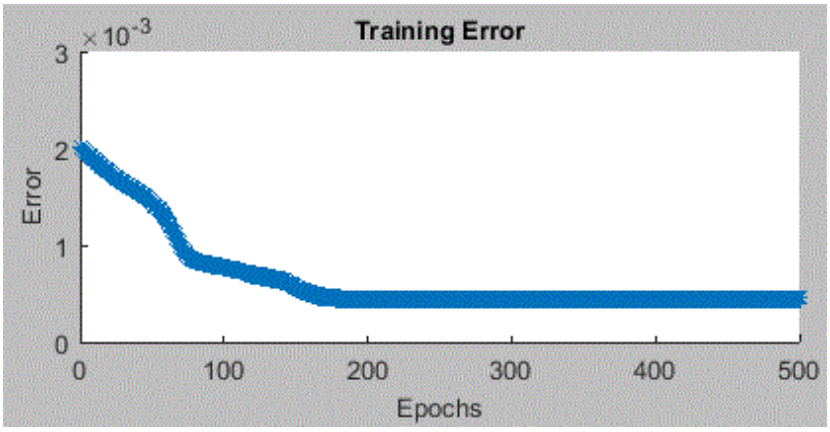

(b)

Fig 4.26 (a) Structure of designed ANFIS model (b) training error

MPPT controller based on neuro fuzzy algorithm is designed using Simulink/MATLAB. The performance of the ANFIS algorithm is analysed for a 680W standalone PV system.

Output power at the load under STC is 664 W as shown in fig 4.27. Voltage tracked by ANFIS algorithm at STC is 47.65 V as shown in fig 4.28. Fig 4.29 gives the duty ratio obtained for maximum power.

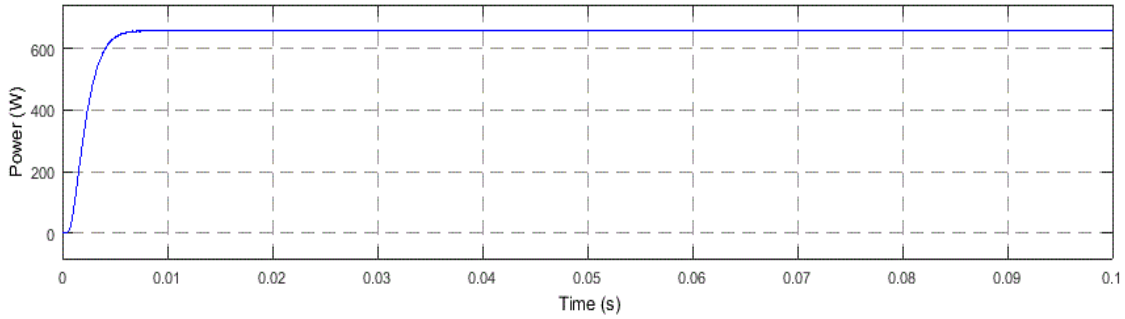

Fig 4.27 Power extracted using ANFIS based algorithm at STC

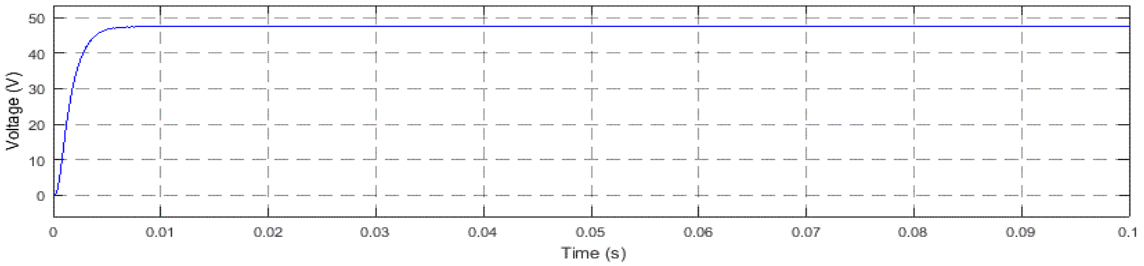

Fig 4.28 Voltage obtained using ANFIS based algorithm at STC

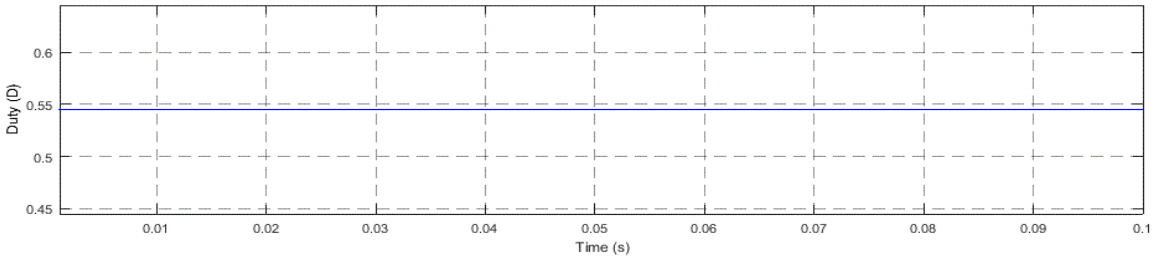

Fig 4.29 Duty ratio obtained at MPP using ANFIS based algorithm at STC

To analyze the effect of irradiation on the power output, the system is operated at varying irradiation and constant temperature of 25^0C. The irradiance is 1000W/m^2 up to 0.1 sec/800W/m^2 from 0.1 to 0.2 sec and 500W from 0.2 to 0.3 sec as shown in fig 4.30. The power extracted by ANFIS MPPT controller is 664W, 543W and 342W respectively.

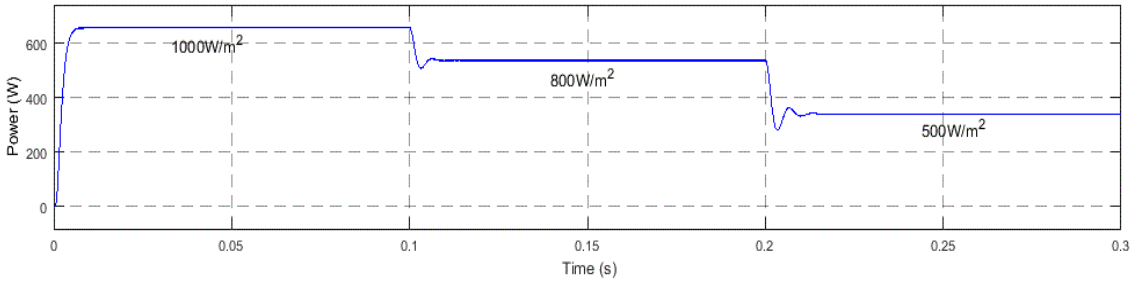

Fig 4.30 Power extracted using ANFIS based algorithm under varying irradiation conditions

To analyze the effect of temperature variation on the power output, the system is operated at varying temperature and constant irradiation of 1000W/m^2. The system is tested at the temperature of 25^{0}C up to 0.1 sec, at 30^{0}C from 0.1 sec to 0.2 sec and at 45^{0}C from 0.2 to 0.3 sec as shown in fig 4.31. The power extracted by ANFIS MPPT controller is 664W, 649W and 600W respectively.

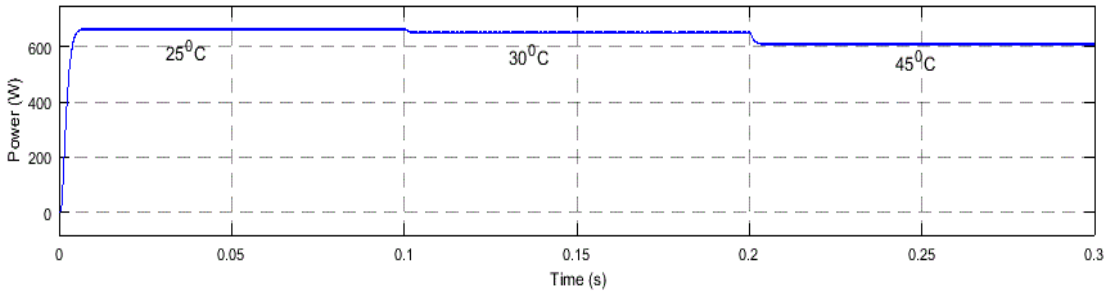

Fig 4.31 Power extracted using ANFIS based algorithm under varying temperature condition

4.3 COMPARISON OF MPPT ALGORITHM

In this chapter various MPPT algorithms are analysed by simulating in MATLAB/Simulink. At irradiation of 1000W/m^2 and temperature of 25^{0}C the power and voltage output of MPPT is shown in table 4.2

TABLE 4.2 COMPARISON OF VOLTAGE AND POWER EXTRACTED BY VARIOUS MPPT ALGORITHMS

	Power extracted at STC(W) with % variation in power.	Voltage obtained at STC(V) with % variation in power
FOCV	652.5 W (±0.6%)	47.25 V(±0.4%)
P&O	660 W (±2%)	47.6 V(± 2.2%)
INC	659 W (± 1.3%)	47.58 V(±1.3%)
FLC	663 W (± 0.5%)	47.65 V(±0.25%)
ANFIS	664 W (±0.5%)	47.65 V(±0.1%)

The power output of the MPPT algorithm at varying irradiation of 1000W/m^2 ,800W/m^2 ,and 500W/m^2 and temperature of 25^0 case is shown in table 4.3

TABLE 4.3 COMPARISON OF PERFORMANCE OF BATTERY FOR VARYING IRRADIATION CONDITIONS

	1000 W/m^2			800 W/m^2			500 W/m2		
MPPT ALGORITHMS	P (W)	Settling time (s)	Overshoot/ Undershoot (W)	P (W)	Settling Time (s)	Overshoot/ Undershoot (W)	P (W)	Settling time (s)	Overshoot/ Undershoot (W)
FOCV	652.5	0.045	10	532	0.02	No u/s	335	0.004	No u/s
P&O	660	0.01	6	533	0.008	53	335	0.01	115
INC	659	0.02	4	533	0.006	56	334	0.008	134
FLC	663	0.005	No o/s	542	0.006	32	342	0.008	60
ANFIS	664	0.005	No o/s	543	0.006	33	342	0.008	60

The power output of the MPPT algorithm at varying temperature of,25^0C,30^0Cand 45^0C and irradiation of 1000W/m^2 are shown in table 4.4

TABLE 4.4 COMPARISON OF PERFORMANCE OF BATTERY FOR VARYING TEMPERATURE CONDITIONS

	25^0C			30^0C			45^0C		
MPPT ALGORITHMS	P (W)	Settling time (s)	Overshoot/ Undershoot (W)	P (W)	Settling Time(s)	Overshoot/ Undershoot (W)	P (W)	Settling time (s)	Overshoot/ Undershoot (W)
FOCV	652.5	0.045	10	619	0.007	No u/s	468	0.007	No u/s
P&O	660	0.01	6	645	0.008	No u/s	595	0.008	No u/s
INC	659	0.02	4	644	0.006	No/u/s	594	0.009	No u/s
FLC	663	0.005	No o/s	648	0.005	No/u/s	597	0.006	No u/s
ANFIS	664	0.005	No o/s	649	0.005	No/u/s	600	0.006	No u/s

The power output for various MPPT algorithm at STC is shown in fig 4.32.

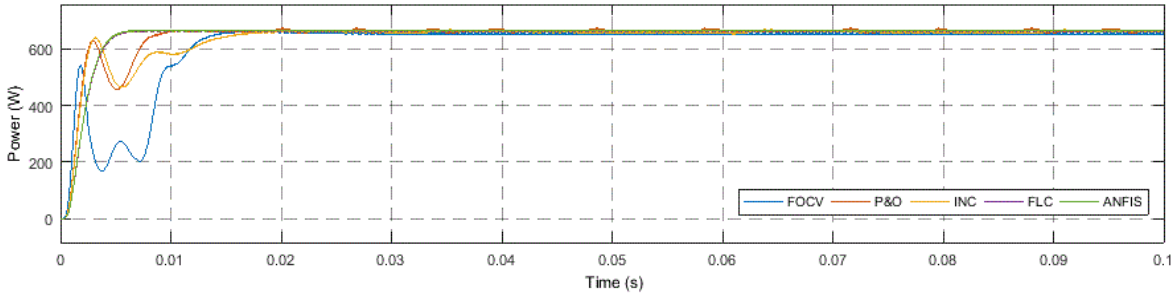

Fig 4.32 Comparison of power extracted by various MPPT algorithms

4.4 CONCLUSION

In this chapter various MPPT algorithms viz. FOCV,P&O,INC,FLC,ANFIS are designed and their performance is compared under various levels of irradiation and temperature. Based on the simulation results of MPPT algorithms following conclusions can be drawn-

a) ANFIS MPPT algorithm extract maximum power from the PV array while FOCV MPPT algorithm extract minimum power from the PV array at STC.

b) The variation in power at MPP is highest in P&O and Incremental conductance algorithm and least in ANFIS.

c) ANFIS algorithm took least time to reach MPP and it is the fastest algorithm.

CHAPTER V
BATTERY CHARGING SYSTEM

INTRODUCTION

In standalone PV system, PV array works only in daytime when sunlight is available. At night or under cloudy conditions PV array failed to provide required power. This makes battery storage system a critical part of standalone PV system. Batteries during charging store the electrical energy in the form of chemical energy and during their discharging the chemical energy generates energy in the form of an electric current at a certain voltage.

There are various methods for charging of a battery such as constant current, constant voltage, constant current-constant voltage etc. Among these methods constant current-constant voltage (CC-CV) method is most widely used method. This method provides fast charging of battery without deteriorating the life of battery. In this chapter design of a battery charging system for a standalone PV system using constant current-constant voltage (CC-CV) method has been presented. For further analysis of battery charging process battery charging systems using AC supply has also been presented. AC based battery chargers find applications as household battery charger and in EVs.

5.2 BATTERY TERMINOLOGY AND VARIOUS CHARGING METHODS

This section describes various definitions and charging methods which are used for battery charging. The terminology described in this section are useful in understanding of battery and it's charging technology.

5.2.1 Definitions [30]

i) Ampere Hour

Ampere hour is given by the product resulting from multiplication of current (A) flowing and time for which current flows in hours, e.g., a battery supplying 5 amperes for 15 hours gives 75 ampere hours.

ii) C rate

C rate of a battery give the rate of discharging of a battery relative to its maximum capacity. For example, 1Ah battery take 1h to discharge at 1C rate. The same battery discharge in 2h at 0.5C rate and in half hour at a rate of 2C.

iii) Nominal Voltage

Nominal voltage is the measured voltage at the mid-point between the full charged and full discharged voltage on a 0.2C discharge rate. The nominal voltage of a battery depends on the chemical composition of battery.

iv) Open Circuit Voltage (OCV)

It is the voltage observed across the battery terminals, during no load conditions. The open-circuit voltage depends on SOC of the battery. As the SOC of the battery decreases the open-circuit voltage also reduces.

v) Gassing

The giving off of hydrogen gas at negatives and oxygen gas at positive plates is known as gassing. The process of gassing begins during charging when battery charged more than 50% [28].

vi) Charge Efficiency

Charge efficiency is defined as the ratio of the ampere-hours delivered during discharge to ampere-hours required to restore 100% state of charge. Its value is calculated in percentage.

vii) Float Charge voltage

It is the voltage required to preserve the battery at a full-state of power while minimizing overcharge. When the battery becomes fully charged a float charge is generally applied. Float charge compensate for leakage charge of the battery [29].

viii) State of Charge (SOC)

It is defined as the ratio of the remaining ampere hours (AH) in a battery in ration of the rated capacity of the battery. It is measured in percentage.

xi) Depth of Discharge (DOD)

It is defined as the product, represented in percentile, obtained by ratio of the ampere-hours delivered during discharge to the rated ampere-hour capacity.

x) Overcharging

It is defined as the continues charging of the battery even after having charged to 100% capacity, or excessive charging than mentioned float charge voltage. It leads to loss of capacity and life cycle of the battery.

xi) Dry-Out

It refers to the complete loss of battery's electrolyte because of gassing. It mainly occurs when a battery is over charged.

xii) End of Life (EOL)

It is the point in the life-span of the battery, when it can only delivers 80% or at reduced capacity than rated.

5.2.2 Battery Charging Techniques [28]

This section describes the various methods of battery charging. Some techniques for charging are-

i). Constant Voltage Charging

It is the simplest form of charging. In this method a constant DC voltage source is used for charging a battery. It allows the maximum current to flow in the battery. As charging of the battery is done at constant voltage, the current in the battery decreases. This leads to large charging time.

ii). Constant Current Charging

In this method of charging a constant current is maintained by varying the voltage during charging process. This method maintains the current to the maximum allowed value. So a faster charging than the constant voltage method is obtained in this method. However, this method has the disadvantage that the battery can overcharge by this method which decreases the overall life of the battery. So to overcome these disadvantages charging by constant current and constant voltage is preferred.

iii). Constant Current-Constant Voltage Charging

This charging method consists of three stages. Primarily, a constant charging current is maintained until the battery voltage reaches a pre-set voltage. During second stage, a constant voltage of maximum battery voltage is maintained until the battery is fully charged as represented in fig 5.1.

In the third and final stage a constant voltage known as the float voltage is maintained across the battery. In this stage a very small current to compensate the self-discharging of battery is generated. This is the most widely used method of faster charging. This method provides overcharging protecting. This method of charging is used in this work.

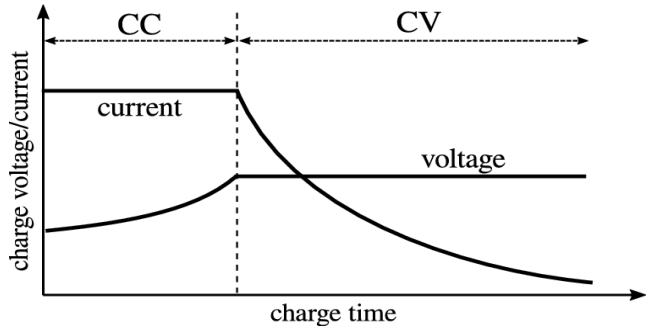

Fig 5.1 Constant current-Constant voltage charging

iv). Pulsed charging

In this charging the battery is charged by pulses of current. The rate of charging of a battery can be increased or decreased by varying the pulse width of current. This charging method has the advantage as high voltage of short duration can be applied in this method without overheating of the battery.

v) IUI Charging

In this charging method initially battery is charged at a constant current (I) rate. As the voltage of the battery reaches a pre-set value, a constant voltage (U) is applied across the battery. The pre-set voltage value of the battery is the voltage at which gassing starts. During constant voltage phase as the battery charges the charging current in the battery decreases and reach another pre-set level. In the third and final phase, a constant current (I) is applied. In this phase battery becomes fully charged and the charger is switched off. This charging method is used for flooded lead acid batteries. This method of charging is not widely used as it pre-set voltage depends on gassing.

5.3 BATTERY CHARGING SCHEME FOR STANDALONE PV SYSTEM

This section describes the design and analysis of lead acid battery charging scheme. A lead acid battery has the advantage of lower cost, lower maintenance, high energy efficiency and low self-discharge rate of the battery [27][30]. In this work constant current-constant voltage charging method is used for charging of the battery. The control strategy used for charging is based on the SOC of the battery. The strategy used consist of three stage in the first stage duty ratio of the DC-DC converter is varied by using INC maximum power tracking algorithm and the next two stages are implemented by using two PI loops in cascade [28]. This ensures safe and faster charging of the battery.

5.3.1 Configuration of the system

The basic configuration of battery charging system by photovoltaic array is given by fig 5.2. The designed charger has a power rating of 160W and voltage of 28.8V is maintained at the output of the converter to obtain a continuous current flow into the battery using the proper control.

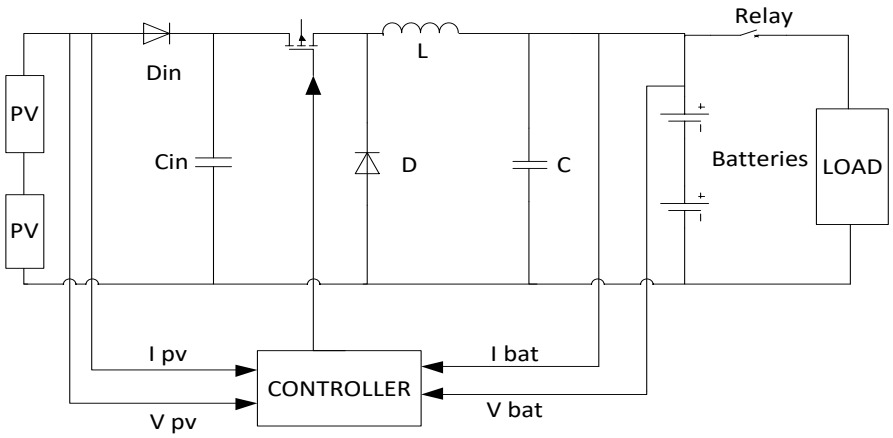

Fig 5.2 Basic configuration of photovoltaic battery charging system.

The PV array used have a capacity of 160 W with maximum power voltage of 35V and maximum current of 5.1 A as shown in table I.

TABLE 5.1 PARAMETERS OF PV MODULE FOR BATTERY CHARGING

PV panel parameter	**Value**
Open circuit voltage V_{oc}	21.3 V
Short circuit current I_{sc}	6.5 A
Cells per module N_s	36
Current at MPP I_{mp}	5.1 A
Voltage at MPP V_{mp}	17.5 V
Power at MPP P_{max}	80 W
R_p	245.76 ohm
R_s	0.2712 ohm
K_v	-0.1230 V/K
K_i	0.0032 A/K
I_0	$2.647*10^{-8}$ A
Series connected modules per string	2
Number of parallel strings	1

The battery bank consists of 2 batteries of 18Ah capacity with a voltage of 24V(12x2) as shown in table 5.2.

TABLE 5.2 BATTERY BANK PARAMETERS

Battery parameter	**Value**
Nominal Voltage (V)	*24V*
Nominal Capacity	36Ah
Max. battery voltage(V_{batmax})	*28.8V*
Min. battery voltage(V_{batmin})	*19.3V*
Float charge voltage$_{(V_{float})}$	*24.46V*
Max. battery current(I_{batmax})	*16A*
Min. battery current(I_{batmin})	*0.4A*

5.3.2 Battery Charging Algorithm

The operation of battery charging consists of 3 stages:

Stage 1 Bulk charge region

In this region the voltage of battery lies between minimum allowed battery voltage ($V_{bat\ min}$) and max. over-load voltage(V_{batmax}). In this stage battery is charged at constant load current by using maximum power point tracking controller. The battery is charged to a level of 80 to 90 percent SOC in this stage [28][29].

Stage 2 Overcharge region

This region of operation is defined when battery voltage reaches the maximum battery voltage (V_{batmax}). In this region, a voltage control takes place where the set point is adjusted to $Vb_{at\text{-}max}$. The control of voltage and current in this region is obtained using PI controllers G_V and G_I respectively and feedback constants H_V and H_I as shown in fig 5.3 [28][[29].

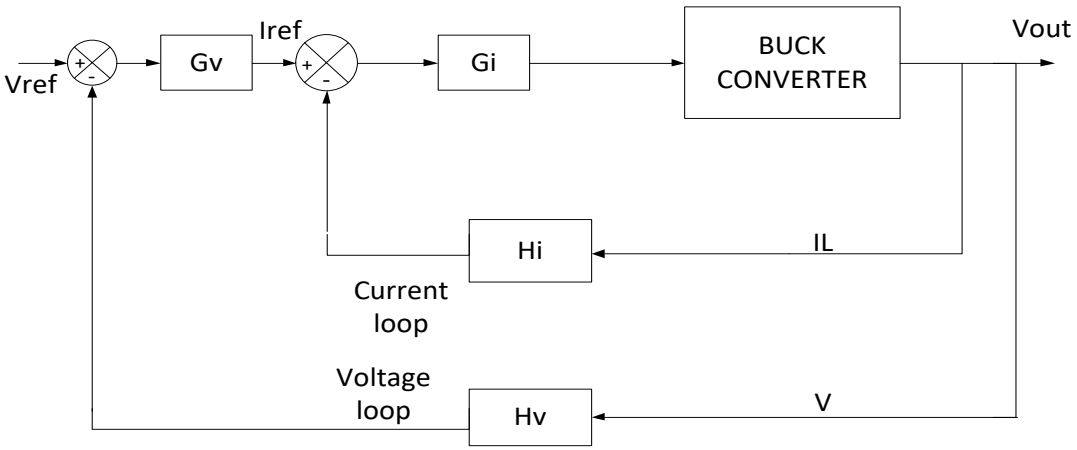

Fig 5.3 Voltage control of battery using PI controllers

Stage 3 Float charge region

In this region of charging the battery is charged at a constant voltage. The constant voltage $V_{bat\text{-}float}$ is maintained as reference voltage in this stage. The battery charging occurs in this region when the current in the battery falls below $I_{bat\text{-}min}$ [32]. The current generated in this stage is used for compensating self-discharge in the battery [31][32]. If the SOC of the battery falls below permitted value, then the battery is disconnected by relay. The flowchart of battery charging control is given by fig 5.4

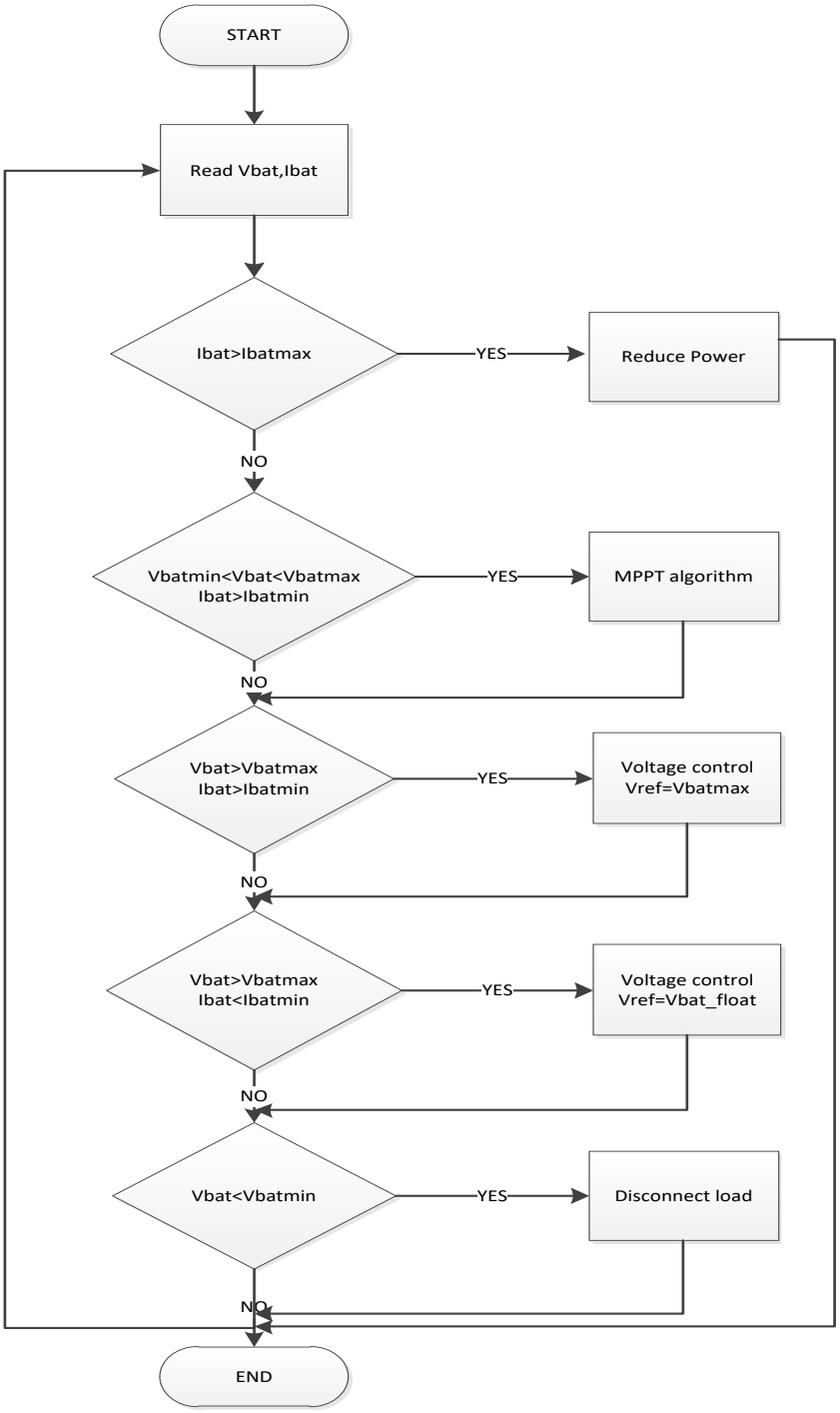

Fig 5.4 Flowchart of Battery charging scheme

5.3.3 Simulation results

The battery charging scheme is designed and simulated using MATLAB/Simulink. Simulation results are shown in fig 5.5 and fig 5.6 for rated supply conditions in constant current (CC) mode charging with initial SOC of 55%. The voltage of the battery increases from 24.02 V to 24.38 V at a constant current of 6.1A in 14 seconds. Fig 5.7 given the

SOC of the battery during the charging time. The battery operates at a duty ratio of 0.67 during constant current (CC) mode of charging as shown in fig 5.8.

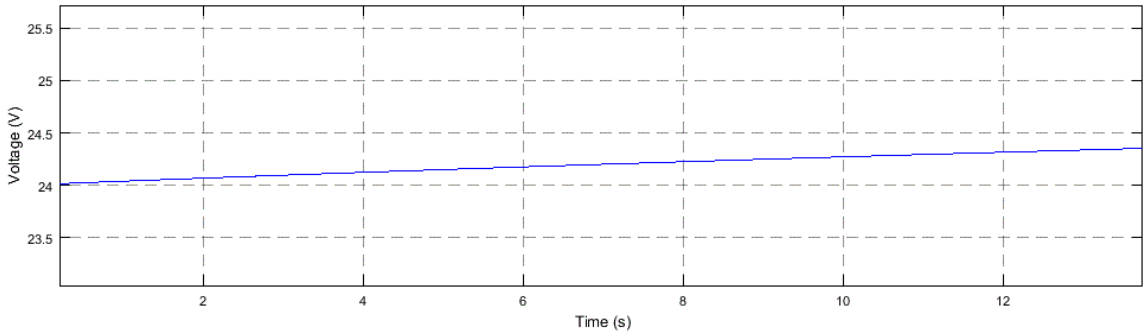

Fig 5.5 Voltage across battery during charging

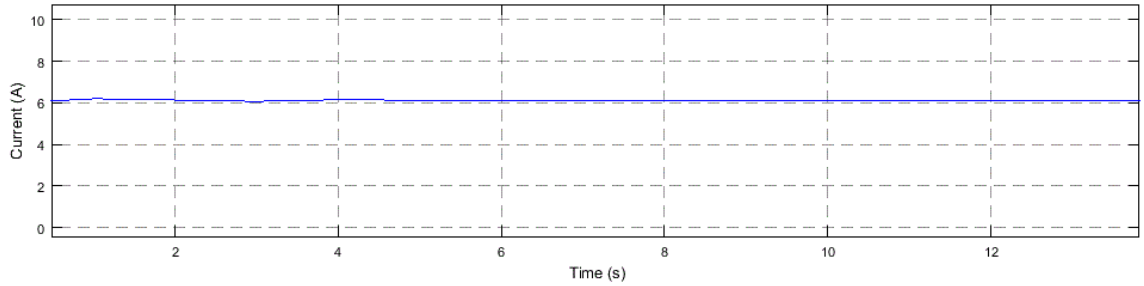

Fig 5.6 Current drawn by the battery during charging

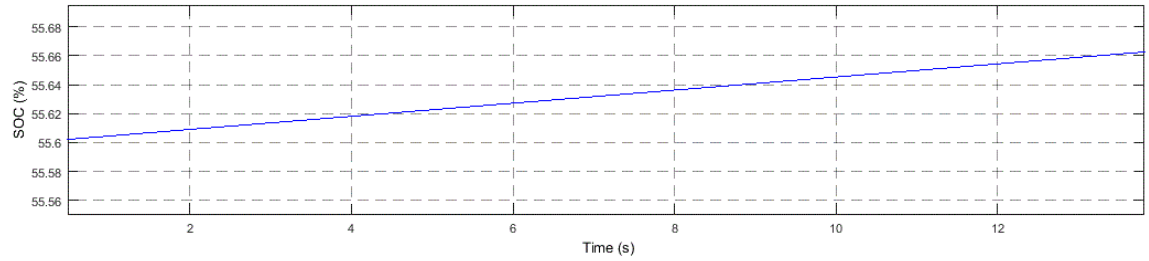

Fig 5.7 SOC of the battery during charging

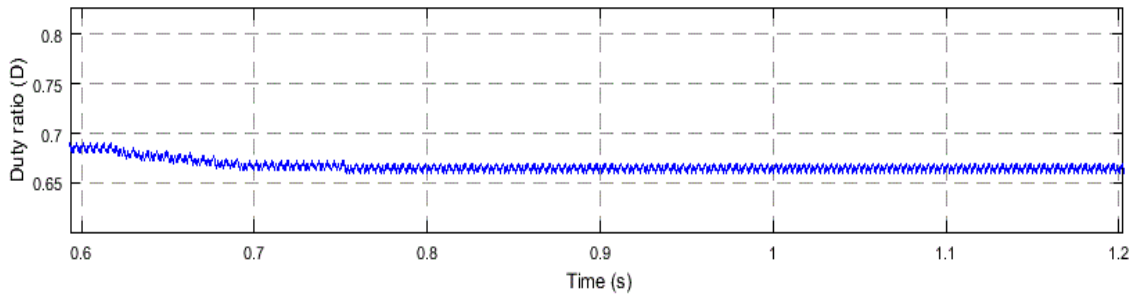

Fig 5.8 Duty ratio during current control stage

5.4 BATTERY CHARGING FROM THE AC SUPPLY (EV BATTERY CHARGER)

This section describes the design of AC based charging scheme for lead acid battery charger. AC to DC chargers consist of diode bridge converter for providing DC charging current to the battery. The diode bridge converter due to its non-linear nature has bad impact on the input power profile. These converters inject harmonics into the AC system. These converters have high THD, voltage distortion and low PF.

To eliminate the problem of low power factor power factor correction (PFC) based converter can be used. A PFC based converter shape the grid current to maintain it in phase with the voltage. A high frequency transformer is used for removing the harmonics present into the current, to protect the battery from harmonics and improving the overall charging performance of the battery.

Sheppard Taylor converter topology was developed by DI Sheppard, BE Taylor in 1983[33]. This converter provides non pulsating current, with low output voltage regulation. This converter consists of two inductors for shaping the input current during the CCM mode of operation and high pf during DCM mode of operation [33][34]. This converter can be used for both continuous and discontinuous mode of operation. A Sheppard Taylor PFC have no control detuning problems. It gives pure sinusoidal current even at zero crossing. This makes it appropriate for input current shaping [35]. This work is based on PFC controller designed by kushwaha et.al[33].

5.4.1 Configuration of converter

The basic configuration of a Sheppard Taylor PFC converter for the EV battery charging purposes is given in fig 5.8. In this work a battery charger of 1KW rating is used to charge the 48 V battery from 230 V AC supply. The voltage at the charger output is maintained as 65V for ensuring proper charging current in the battery. The current in the battery is controlled using proper PI controllers.

5.4.2 Operating stages

In first stage, switches S_1 and S_2 are ON and inductor L1 is charging and energy of the capacitor C1 is available to the output stage.

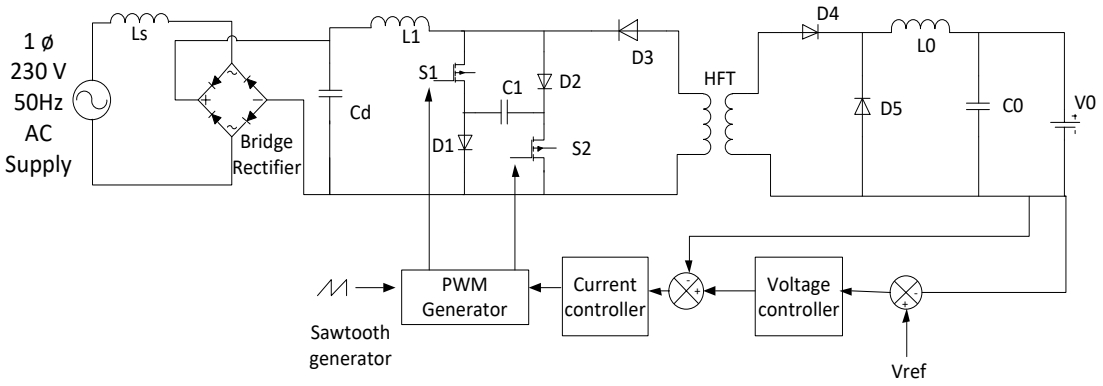

Fig 5.9 Configuration of Sheppard Taylor converter [33]

In the second stage switches S_1 and S_2 are OFF and the input inductor L_1 discharges through diodes D_1 and D_2 and the storage capacitor C_1 start charging.

In the third stage, inductor L_1 becomes fully discharged and the output inductor supplies the current to the battery through freewheeling diode.

5.4.3 Design of converter parameters:

a) Duty cycle (D)

A buck boost converter is used for varying the output current and voltage. Duty ratio of converter is given by equation (5.5)

$$D = \frac{Vo}{\left(\frac{N2}{N1}\right)\sqrt{2}Vs+Vo} \tag{5.5}$$

$$= \frac{65}{0.656*\sqrt{2}*220+65} = 0.172$$

Where V_o is Output voltage, V_s is Source voltage, N_1 is number of primary turns of HFT and N_2 gives number of secondary turns of HFT.

b) Input inductor design (L_1)

Input inductor is selected to obtain discontinuous current in one cycle at a frequency of 50KHz.The value of input inductor is given by equation (5.6).

$$L_1 = \frac{D(V_{c1}+V_1)}{f_s*I_{L1}} \tag{5.6}$$

$$= \frac{0.2(330\ 198)}{50000*(1000\ /198)} = \quad 418.2\mu H$$

Where V_{c1} is voltage across storage capacitor, $V_1$is voltage output of bridge rectifier, f_s is Switching frequency which is taken as 50kHz and I_{L1} is the current in input inductor.

c) Storage capacitor design (C_1)

This capacitor is used for tuning the output of converter for zero crossing at the input. The value of the capacitor can be obtained by using equation (5.7)

$$C_1 = \frac{V_0 D}{\Delta V_{c1} f_s R_0} \tag{5.7}$$

$$= \frac{65*0.2}{0.1*330*50000*\frac{65^2}{1000}} = 1.864\mu F$$

Where V_0 is Voltage output, R_0 is load resistance and ΔV_{c1} is ripple voltage of V_{c1} which is taken as 10% of V_{c1}.

d) Output inductor design (L_0)

Output inductor is used to maintain continuous current at the output for given DC link voltage. The value of Output inductor is given by equation (5.8)

$$L_{0,min} = \frac{V_0(1-D)^2}{2I_0 D f_s}\left(\frac{N_1}{N_2}\right)^2 \tag{5.8}$$

$$= \frac{65*(1-0.2)^2}{2*\left(1000/65\right)*50000*0.2} = 313.69\mu H$$

Where I_0 = Output current, N_1 = Number of primary turns of HFT, N_2 = Number of secondary turns of HFT, f_s = Switching frequency. A value more than $L_{0,\,min}$ is used for output inductor. This work uses output inductor of 350 µH.

e) DC link capacitor design (C_0)

The value of dc link capacitor is calculated based on the ripple required at the output. For a 10% ripple in output voltage the value of capacitor is given by equation (5.9).

$$C_0 = \frac{I_0}{2\omega\Delta V_0} \tag{5.9}$$

$$= \frac{15.38}{(2*314*.1*65)} = 3.77mf$$

Where I_0 is output current, ΔV_0 gives variation in output voltage which is taken as 10% of V_0 and ω is operating frequency which is taken as 314.15 rad/s.

f) Input filter capacitance design (C_f)

Filter capacitance is used to eliminate higher order harmonics in the system. The value of input filter capacitance can be given by equation (5.10).

$$C_{f,max} = \frac{I_{pk}}{\omega V_m} tan\theta \tag{5.10}$$

$$= \frac{100\sqrt{2}/220}{314*220\sqrt{2}}\tan 1^0 = 1149\ nF$$

Where I_{pk} is maximum value of source current, V_m is maximum value of source current, Θ is fundamental displacement angle and ω gives operating frequency=314.15 rad/s.A value less than the $C_{f,max}$ is used as a filter capacitance. The present work use 1000nF as the filter capacitance.

g) Source inductance design (Ls)

Supply inductance is used for maintaining a sinusoidal source current. Its value is given by equation (5.11).

$$L_s = 0.02\left(\frac{1}{\omega}\right)\frac{{V_s}^2}{P} \tag{5.11}$$

$$= \frac{220^2 * 0.02}{314 * 2000} = 4.6\text{mH}$$

Where ω is the operating frequency which is given by 314.15rad/s,V_s is the source voltage and P is the output power.

5.4.4 Charging control

The battery charge controller analysed use PI controllers to control the charging. These controllers control the switches of converter that regulates the current and voltage at the output. These controllers operate the converter.in the constant current mode or constant voltage mode. Initially battery is operated in constant current mode and current PI controller generate the duty ratio based on reference current. When the battery reaches a defined voltage, the control changes to constant voltage [35][36][37]. The voltage PI controller produce control signal by comparing the battery voltage with reference voltage during this mode.

5.4.5 Simulation results

Simulation results for the designed controller are shown in fig 5.10-fig 5.15 in constant current mode charging with initial SOC of 61%. The source voltage and current waveform are given by fig 5.9 and fig 5.10. Output voltage waveform is given by fig 5.12

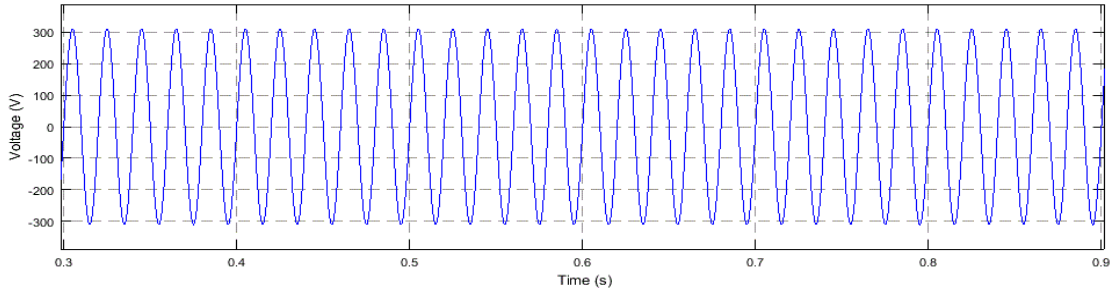

Fig 5.10 Source voltage waveform

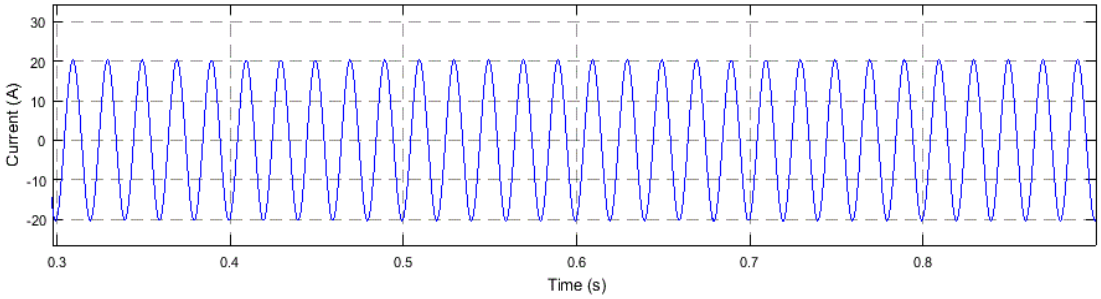

Fig 5.11 Source current waveform

The SOC of battery is shown in fig 5.13.

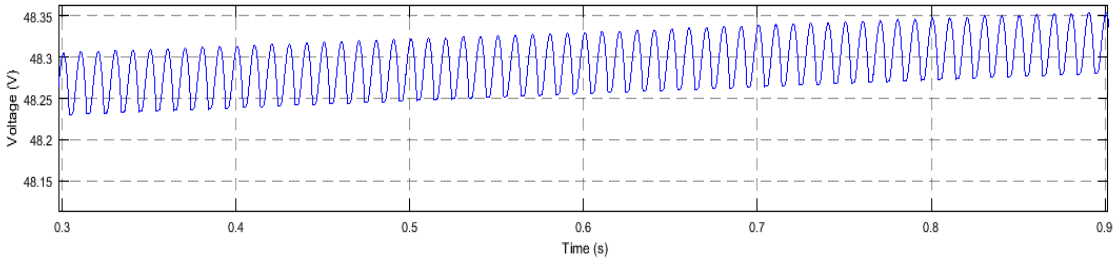

Fig 5.12 Battery voltage waveform

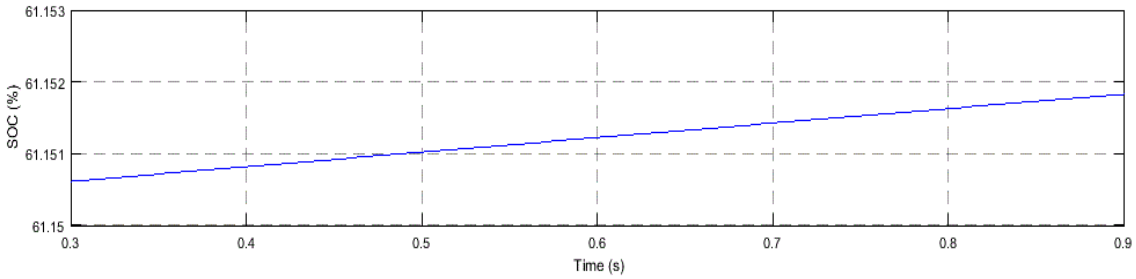

Fig 5.13 Battery SOC (in percentage) change for rated supply

To analyse the harmonics injected in the source current by the battery charger, the THD of the source current is calculated. As shown in fig 5.14 THD of the source current is found to be 0.70% which is well below, IEC 61000-3-2 PQ standard.

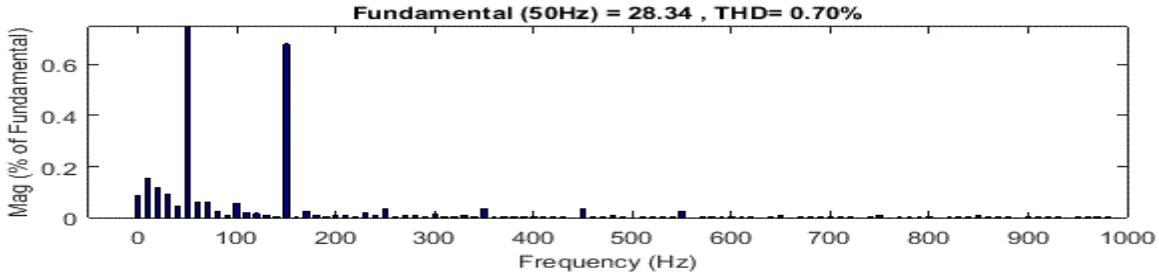

Fig 5.14 Harmonics in supply current due to battery charging

5.5 CONCLUSION

This chapter describe the charging of the battery for standalone PV system and battery charging when grid is connected. The designed battery charging scheme successfully charge the battery using constant current and constant voltage method of charging.

CHAPTER VI

CONCLUSION AND FUTURE SCOPE OF WORK

This work includes the modelling and simulation of standalone solar PV system for dc loads. The Power versus Voltage characteristics and Current versus Voltage characteristics of the given solar PV array is plotted and it is observed that the PV array exhibits non-linear characteristics. PV power output varies with the variation in the solar irradiation and temperature. Therefore, MPPT algorithm is used to track the maximum power point of the PV array according to the given temperature and irradiation. Buck converter along with MPPT capabilities is used to reduce the PV output voltage to the required voltage level. Five different MPPT algorithms namely FOCV, P&O, INC, FLC and ANFIS are designed and developed for the designed PV system. The performance of these algorithms is analysed using MATLAB/Simulink. The ANFIS MPPT algorithm gives best results in extracting power from the designed PV array.

Energy storage is an integral part of a standalone PV system. In the present work, a battery charging scheme for a standalone PV system has been designed. The charging algorithm is based on CC-CV or 3 step charging. The simulation results show the effectiveness of designed scheme. Further the grid based battery charging system is also designed for Electric vehicle application and simulation results are presented. The source side current is maintained at unity power factor with THD within IEEE standard limits.

6.2 FUTURE SCOPE

Further research works may include the analysis of the MPPT algorithm performance under partial shading condition. The designed battery charging schemes can be implemented experimentally. The interfacing of standalone PV system with the grid can be analysed.

REFERENCES

[1] "International Energy Outlook, 2017", U.S. Energy Information Administration.

[2] Chandra, Yogender Pal, Arashdeep Singh, Vikas Kannojiya, and J. P. Kesari. "Solar Energy a Path to India's Prosperity." *Journal of The Institution of Engineers (India): Series C*: 1-8

[3] Sharma, Deepak, and Pooja Khurana. "SOLAR POWER: Challenges, Mission and Potential of Solar Power in India." *Target* 2022 (2018): 13.

[4] Rathore, Pushpendra Kumar Singh, Durg Singh Chauhan, and Rudra Pratap Singh. "Decentralized solar rooftop photovoltaic in India: On the path of sustainable energy security." *Renewable Energy* (2018).

[5] Villalva, Marcelo Gradella, Jonas Rafael Gazoli, and Ernesto Ruppert Filho. "Comprehensive approach to modeling and simulation of photovoltaic arrays." *IEEE Transactions on power electronics* 24, no. 5 (2009): 1198-1208.

[6] Zadeh, Mahdi Jedari Zare, and Seyed Hamid Fathi. "A new approach for photovoltaic arrays modeling and maximum power point estimation in real operating conditions." *IEEE Transactions on Industrial Electronics* 64, no. 12 (2017): 9334-9343.

[7] Augustin McEvoy, Tom Markvart and Luis Castaner, "Practical Handbook of Photovoltaics-Fundamentals and Applications", Second Edition, Elsevier, Wyman Street, USA, 2012

[8] Baharudin, Nor Hanisah, Tunku Muhammad Nizar Tunku Mansur, Fairuz Abdul Hamid, Rosnazri Ali, and Muhammad Irwanto Misrun. "Topologies of DC-DC Converter in Solar PV Applications." *Indonesian Journal of Electrical Engineering and Computer Science* 8, no. 2 (2017): 368-374.

[9] Putri, Ratna Ika, Muhammad Rifa'i, and S. Adhisuwiginjo. "Design of Buck Converter For Photovoltaic System Applications." In *Proceeding Conference on Applied Electromagnetic Technology AEMT*. 2015.

[10] Tucker, Carl William. "A study of photovoltaic cells." *The Journal of Physical Chemistry* 31, no. 9 (1927): 1357-1380.

[11] Chapin, Calvin Fuller, and Gerald Pearson. "Great Ideas Changing the World." (1953).

[12] Alharbi, Fahhad H., and Sabre Kais. "Theoretical limits of photovoltaics efficiency and possible improvements by intuitive approaches learned from photosynthesis and quantum coherence." *Renewable and Sustainable Energy Reviews* 43 (2015): 1073-1089.

[13] "Modeling and simulation of photovoltaic module and array based on one and two diode model using Matlab/Simulink." *Energy Procedia* 74 (2015): 864-877.

[14] Humada, Ali M., Mojgan Hojabri, Saad Mekhilef, and Hussein M. Hamada. "Solar cell parameters extraction based on single and double-diode models: A review." *Renewable and Sustainable Energy Reviews* 56 (2016): 494-509.

[15] Manju, B. Sree, R. Ramaprabha, and B. L. Mathur. "Modelling and control of standalone solar photovoltaic charging system." In *Emerging Trends in Electrical and Computer Technology (ICETECT), 2011 International Conference on*, pp. 78-81. IEEE, 2011.

[16] Gosumbonggot, Jirada. "Maximum power point tracking method using perturb and observe algorithm for small scale DC voltage converter." *Procedia Computer Science* 86 (2016): 421-424.

[17] Sahu, Himanshu Sekhar, Sisir Kumar Nayak, and Sukumar Mishra. "Maximizing the power generation of a partially shaded PV array." *IEEE journal of emerging and selected topics in power electronics* 4, no. 2 (2016): 626-637.

[18] Sera, Dezso, Laszlo Mathe, Tamas Kerekes, Sergiu Viorel Spataru, and Remus Teodorescu. "On the perturb-and-observe and incremental conductance MPPT methods for PV systems." *IEEE journal of photovoltaics* 3, no. 3 (2013): 1070-1078.

[19] Putri, Ratna Ika, Sapto Wibowo, and Muhamad Rifa'i. "Maximum power point tracking for photovoltaic using incremental conductance method." *Energy Procedia* 68 (2015): 22-30.

[20] Tey, Kok Soon, and Saad Mekhilef. "Modified incremental conductance MPPT algorithm to mitigate inaccurate responses under fast-changing solar irradiation level." *Solar Energy* 101 (2014): 333-342.

[21] Algazar, Mohamed M., Hamdy Abd El-Halim, and Mohamed Ezzat El Kotb Salem. "Maximum power point tracking using fuzzy logic control." *International Journal of Electrical Power & Energy Systems* 39, no. 1 (2012): 21-28.

[22] Gupta, Ankit, Pawan Kumar, Rupendra Kumar Pachauri, and Yogesh K. Chauhan. "Performance analysis of neural network and fuzzy logic based MPPT techniques for solar PV systems." In *Power India International Conference (PIICON), 2014 6th IEEE*, pp. 1-6. IEEE, 2014.

[23] Murtaza, Ali F., Hadeed Ahmed Sher, Marcello Chiaberge, Diego Boero, Mirko De Giuseppe, and Khaled E. Addoweesh. "Comparative analysis of maximum power point tracking techniques for PV applications." In Multi Topic Conference (INMIC), 2013 16th International, pp. 83-88. IEEE, 2013.

[24] Gules, Roger, Juliano De Pellegrin Pacheco, Hélio Leães Hey, and Johninson Imhoff. "A maximum power point tracking system with parallel connection for PV stand-alone applications." *IEEE Transactions on Industrial Electronics* 55, no. 7 (2008): 2674-2683.

[25] Alajmi, B., K. Ahmed, S. Finney, and B. Williams. "Fuzzy logic controlled approach of a modified hill climbing method for maximum power point in microgrid stand-alone photovoltaic system." *IEEE Transactions on Power Electronics* 26, no. 4 (2011): 1022-1030.

[26] Lin, Whei-Min, Chih-Ming Hong, and Chiung-Hsing Chen. "Neural-network-based MPPT control of a stand-alone hybrid power generation system." *IEEE transactions on power electronics* 26, no. 12 (2011): 3571-3581.

[27] Glavin, M.E., Chan, P.K., Armstrong, S. and Hurley, W.G., 2008, September. A stand-alone photovoltaic supercapacitor battery hybrid energy storage system. In *Power Electronics and Motion Control Conference, 2008. EPE-PEMC 2008. 13th*(pp. 1688-1695). IEEE.

[28] López, Julio, S. I. Seleme Jr, P. F. Donoso, L. M. F. Morais, P. C. Cortizo, and M. A. Severo. "Digital control strategy for a buck converter operating as a battery charger for stand-alone photovoltaic systems." *Solar Energy* 140 (2016): 171-187.

[29] Hussein, Ala A., and Abbas A. Fardoun. "Design considerations and performance evaluation of outdoor PV battery chargers." *Renewable Energy* 82 (2015): 85-91.

[30] Kushwaha, Radha, and Bhim Singh. "An EV battery charger based on PFC Sheppard Taylor Converter." In *Power Systems Conference (NPSC), 2016 National*, pp. 1-6. IEEE, 2016.

[31] Yilmaz, Murat, and Philip T. Krein. "Review of battery charger topologies, charging power levels, and infrastructure for plug-in electric and hybrid vehicles." *IEEE Transactions on Power Electronics* 28, no. 5 (2013): 2151-2169.

[32] Subotic, Ivan, Nandor Bodo, Emil Levi, and Martin Jones. "Onboard integrated battery charger for EVs using an asymmetrical nine-phase machine." *IEEE Transactions on industrial electronics* 62, no. 5 (2015): 3285-3295.

[33] Gautam, Deepak S., Fariborz Musavi, Murray Edington, Wilson Eberle, and William G. Dunford. "An automotive onboard 3.3-kW battery charger for PHEV application." *IEEE Transactions on Vehicular Technology* 61, no. 8 (2012): 3466-3474.

[34] Bai, Hua, Allan Taylor, Wei Guo, G. Szatmari-Voicu, N. Wang, J. Patterson, and J. Kane. "Design of an 11 kW power factor correction and 10 kW ZVS DC/DC converter for a high-efficiency battery charger in electric vehicles." *IET Power Electronics* 5, no. 9 (2012): 1714-1722.

[35] Hu, Xiaosong, Changfu Zou, Caiping Zhang, and Yang Li. "Technological developments in batteries: a survey of principal roles, types, and management needs." IEEE Power and Energy Magazine 15, no. 5 (2017): 20-31.

[36] Chiang, S. J., Hsin-Jang Shieh, and Ming-Chieh Chen. "Modeling and control of PV charger system with SEPIC converter." *IEEE Transactions on Industrial Electronics* 56, no. 11 (2009): 4344-4353.

[37] Fakham, Hicham, Di Lu, and Bruno Francois. "Power control design of a battery charger in a hybrid active PV generator for load-following applications." *IEEE Transactions on Industrial Electronics* 58, no. 1 (2011): 85-94.

[38] Musavi, Fariborz, Murray Edington, Wilson Eberle, and William G. Dunford. "Evaluation and efficiency comparison of front end AC-DC plug-in hybrid charger topologies." *IEEE Transactions on Smart grid* 3, no. 1 (2012): 413-421.

APPENDICES

APPENDIX I Kyocera KD135GX-LFBS module datasheet

APPENDIX II Simulink model PV based charger

APPENDIX III Simulink model of battery charger from AC supply

II Simulink model PV based charger

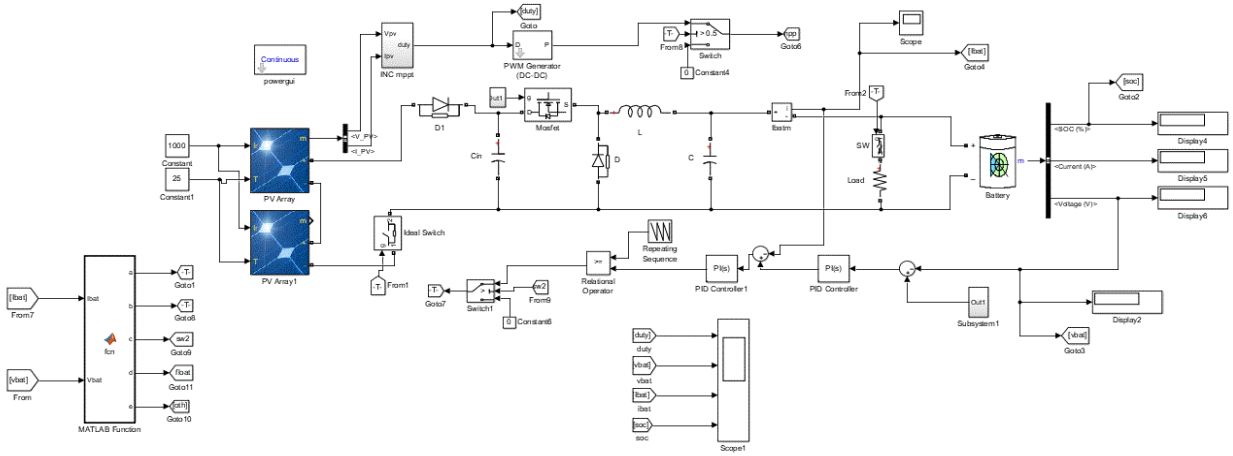

III Simulink model of battery charger from AC supply